in tubule dilation. Renal tubular epithelial cell proliferation increases significantly and renal tubules start to dilate at 3 days after UUO [20, 21]. The extent of tubule dilation is related to the progressive increase in tubular epithelial cell number caused by proliferation. This process ultimately results in the fracture of the tubular basement membrane of the dilated renal tubules. In damaged kidneys, tubular epithelial cells trans-differentiate into mesenchymal cells that express α-smooth muscle actin (α-SMA) in response to kidney inflammation. These cells enter the tubular interstitium through the broken tubular basement membrane [22, 23]. The trans-differentiated tubular epithelial cells further differentiate into myofibroblasts (i.e., fibroblasts expressed α-SMA) in the interstitium. Concurrently, macrophages in the renal interstitium release several cytokines, including epidermal growth factor (EGF), platelet-derived growth factor (PDGF), and fibroblast growth factor-2 (FGF-2), which activate fibroblasts. The interstitial myofibroblasts undergo hyperproliferation because of their high cell responsiveness, resulting in irreversible progression of renal interstitial fibrosis (Fig. 1). There are many reports of establishing UUO in knockout mice and the roles of many cell cycle-related molecules in renal damage have been investigated in UUO kidneys [24].

Another experimental model of chronic progressive glomerulonephritis can be induced in rats by repeated injections of ATS. In this model, irreversible glomerulosclerosis and tubulointerstitial fibrosis are induced after the second ATS injection and are associated with a gradual decline of renal function [25–27]. Alternatively, chronic renal failure can also be studied in the 5/6 nephrectomy model [28, 29] and in diabetic nephropathy [30, 31].

Signal transduction pathways involved in renal damage

Transforming growth factor-β1 (TGF-β1)/Smad pathway

TGF-β1 is a multifunctional signaling protein that regulates cell cycle, apoptosis, differentiation, and extracellular matrix accumulation [32]. TGF-β1 also has a significant role in the progression of renal fibrosis in clinical and experimental kidney diseases [25, 33]. Following the onset of nephropathy, TGF-β1 is released from macrophages in the damaged renal interstitium and influences the tubular epithelial cells. The damaged tubular epithelial cells also release TGF-β1, which exacerbates renal damage. TGF-β1 was also reported to stimulate the epithelial-mesenchymal transition (EMT) [34–36]. Finally, tubular epithelial cells that acquire a fibroblastic phenotype via EMT migrate into the interstitium, probably through the ruptured tubular basement membrane. TGF-β1 also promotes the differentiation of interstitial fibroblasts to myofibroblasts and their production of extracellular matrix [37, 38]. The accumulation of extracellular matrix in the tubulointerstitium and in the glomerulus is also stimulated by TGF-β1. Conversely, TGF-β1 promotes apoptosis of tubular epithelial cells via a p38 mitogen-activated protein kinase-dependent mechanism [39, 40]. Overall, upregulation of TGF-β1 contributes to EMT during renal fibrosis and apoptosis, and it induces the progression of nephropathy.

In terms of the TGF-β1 signaling pathway, Smad proteins play important roles as signal transducers downstream of TGF-β1 receptors [41, 42]. TGF-β1 binds to the TGF-β type II receptor, which recruits and phosphorylates the TGF-β type I receptor, ALK5. In turn, ALK5 phosphorylates Smad2 and Smad3, which then bind to Smad4 [43, 44]. The resulting complexes can then enter the nucleus [45–47]. Another Smad, Smad7, has an inhibitory role in the TGF-β1 signaling pathway [48]. It was also reported that chronic progressive renal injury can be suppressed by inhibiting the TGF-β/Smad axis using an anti-TGF-β antibody [27]. Although TGF-β1 signaling is also mediated by ALK1, another TGF-β type I receptor that phosphorylates Smad1/5 [49], little is known about the roles of the ALK1/Smad1/5 pathway in renal injury. It was also suggested that TGF-β promotes translocation of Skp2 into the nucleus, where it is degraded by the anaphase-promoting complex/cyclosome (APC/C)-Cdh1 E3 ligase. In addition, TGF-β decreases Cks1 mRNA expression, which allows p27 to accumulate following G1 arrest [50–52]. Taken together, these findings indicate that TGF-β is an important upstream signal that regulates the Skp2/p27 axis.

Tumor necrosis factor-α (TNF-α)/nuclear factor (NF)-κB pathway

TNF-α is a multifunctional cytokine that induces a wide range of cellular responses, including proliferation, differentiation, and activation of apoptosis [53]. TNF-α is produced by activated macrophages, and it stimulates the proliferation and apoptosis of renal tubular epithelial cells and interstitial cells in renal injury [54–56]. TNF-α binds to two different TNF receptors (TNFR), type 1 and type 2 receptors [57, 58]. On binding of TNF-α to TNFR1, TNFR1 recruits TNFR-associated death domain (TRADD) as an adaptor protein thorough death domain within 2 min. In turn, TRADD serves as an assembly platform protein to arborize TNFR1 signaling between apoptosis and anti-apoptosis/proliferation. TRADD recruits Fas-associated death domain protein (FADD) to its death domain and activates the Caspase-8/-3 cascade to induce apoptosis [59, 60]. TRADD also recruits TNF-associated factor 2 (TRAF2) and receptor interaction protein (RIP), leading to the activation of NF-κB, which has anti-apoptotic effects [57, 61]. It has been reported that the TNFR1/TRADD/TRAF2/RIP complex is produced more

quickly than the TRADD/FADD complex because of the antagonistic effects of the TNFR1/TRADD/FADD on apoptosis signaling pathways.

TNF-α can also bind to TNFR2, which recruits TRAF2 and activated NF-κB [62]. However, binding of TNF-α to TNFR2 promotes TRAF2 degradation through the ubiquitin-dependent proteasome pathway, resulting in the suppression of NF-κB activation by inhibition of TRADD/TRAF2/RIP complex formation. In addition, TNF-α decreases TRADD protein levels by enhancing its ubiquitin-dependent degradation in obstructive renal damage [20]. In the kidneys, it was reported that renal damage caused by cisplatin was less severe in TNFR2-deficient mice than in TNFR1-deficient mice [67]. However, renal damage in UUO mice was less severe in TNFR1-deficient mice than in TNFR2-deficient mice [63]. It was also reported that a reduction of TRADD inhibits TNFR1 signaling and that TNFR1-mediated TNF-α signaling may transfer to TNFR2 signaling in UUO mice [20]. Another report revealed that the two TNFRs may act collaboratively to regulate signal transduction [64, 65]. However, it has been unclear how TNFR2 regulates the TNF-α signaling pathway until now.

The transcription factor NF-κB, a downstream factor of TNF-α, is activated in renal damage and controls the activation of many genes related to inflammation [66, 67]. NF-κB is an inductive homo- or heterodimeric transcription factor composed of the Rel family members of DNA-binding proteins, including p50/p105 (NF-κB1), p52/p100 (NF-κB2), RelA (p65), RelB, and c-Rel [68]. Activated NF-κB behaves as an important regulator of inflammation and immune responses by mediating the expression of pro-inflammatory genes, including cytokines, chemokines, growth factors, and adhesion molecules, which are implicated in the progression of renal inflammatory disease [69, 70]. The downstream targets of NF-κB are also important regulators of cell proliferation. For example, the IκB-inducing kinase (IKK)-regulated signaling pathway accelerates cell proliferation. Furthermore, IKK-α, an essential component of the NF-κB pathway, affects many physiologic activities in both healthy and disease states [71], including mammary epithelial cell proliferation [72]. In renal injury, NF-κB stimulates tubular epithelial cells and fibroblasts, and induces their proliferation and differentiation, which ultimately promote the progression of renal fibrosis [73]. It was reported that the NF-κB pathway regulates Skp2 expression [74, 75]. As described below, we have suggested that TNF-α stimulates Skp2 and Cks1 mRNA expression via the NF-κB pathway in chronic nephropathy [76]. Therefore, TNF-α is likely to participate in Skp2/Cks1-dependent degradation of p27 as a precipitating factor of chronic nephropathy.

Role of the Skp2/p27 axis in the progression of renal damage

Skp2

The SCF/Skp2 ubiquitin ligase complex targets several important regulator proteins that control the cell cycle, including p27, p21, p57, cyclin E, cyclin A, and cyclin D1 [77], by promoting their degradation via the ubiquitin proteasome-dependent pathway. In this way, Skp2 ubiquitin ligase promotes cell cycle progression to the S-phase by stimulating the degradation of negative cell cycle regulators, such as the CKI p27 [78, 79] (Fig. 2). Moreover, it has been reported that Kip1 ubiquitination-promoting complex (KPC) [80] and Pirh2 [81] act as E3 ligases for p27, whereas it has not been clarified whether p27 is accumulated in their

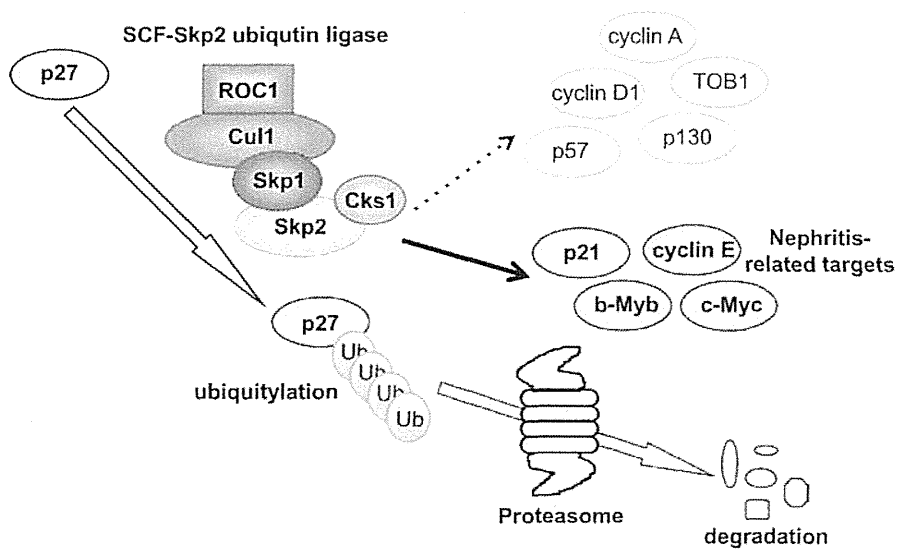

Fig. 2 The mechanism of p27 degradation by Skp2 E3 ubiquitin ligase. SCF (Skp1/Cul1/Skp2 as F-box) ubiquitin ligase induces p27 degradation by a proteasome-dependent pathway. Cks1 is an essential cofactor for p27 degradation by SCF/Skp2 that induces rigid binding between Skp2 and p27. Conversely, Skp2 has multiple targets and may also regulate p21, cyclin E, b-Myb, and c-Myc protein levels in unilateral ureteral obstruction (UUO). However, Skp2 did not affect the regulation of cyclin A, cyclin D1, TOB1, p57, or p130 in UUO kidneys

knockout mice. In human cancers, it was demonstrated that Skp2 overexpression stimulates the degradation of p27, indicating that Skp2 overexpression facilitates accelerated tumor growth and malignant potential [77]. However, the proteins that are targeted by Skp2 for degradation in specific biological processes or diseases have not been fully characterized.

We previously reported that Skp2 mRNA expression was increased in UUO kidneys in the early stages of renal damage and that the progression of tubulointerstitial fibrotic damage in UUO kidneys is attenuated in Skp2-deficient mice [26]. Furthermore, as described above, the mRNA and protein levels of Skp2 were increased in the ATS model of chronic nephropathy in rats [76]. It was reported that the NF-κB signaling pathway regulates the Skp2 promoter in cultured cells [74, 75]. TNF-α was reported to enhance mRNA expression of Skp2 in a normal rat epithelial kidney cell line (NRK) but not in control cells, which suggests that TNF-α facilitates the induction of Skp2 in nephropathy. In damaged kidneys, exposure to TNF-α significantly increased in cytoplasm of tubular epithelial cells. RelB and p52 proteins are known as NF-κB, and they are mainly seen in the nuclei of tubular epithelial cells. Skp2 is also expressed in the nuclei of tubular epithelial cells, similar to RelB and p52. Skp2 and RelB are colocalized in renal damage [76]. These data suggest that Skp2 is induced by the TNF-α/RelB/p52 signaling pathway in the early stages of renal injury and facilitates ubiquitin-dependent degradation of p27 in tubular epithelial cell proliferation and in the progression of chronic nephropathy (Fig. 3).

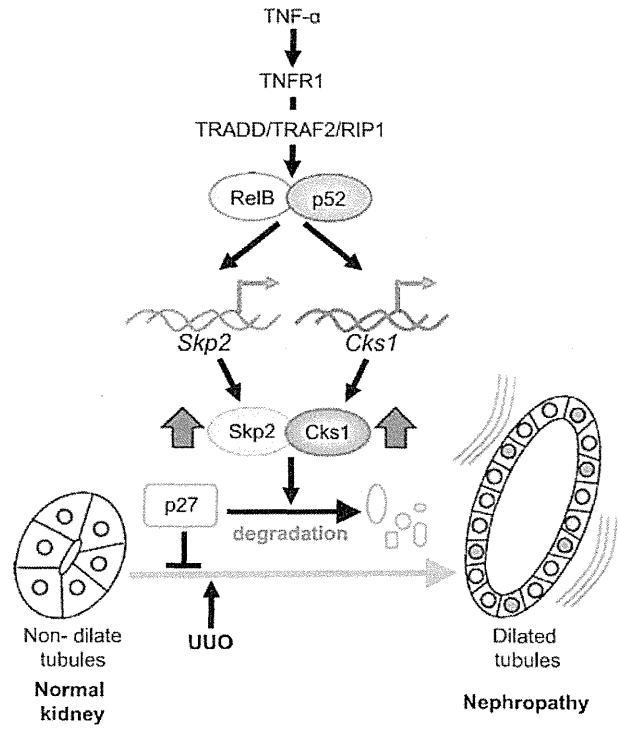

Fig. 3 Skp2/Cks1 is induced by the TNF-α/NF-κB signaling pathway in nephropathy. In normal kidneys, tubular epithelial cells highly express p27 in the quiescent phase of the cell cycle. Following renal damage, TNF-α activates RelB/p52, known as NF-κB, via TNFR1. The activated RelB/p52 complex induces the expression of both Skp2 and Cks1 in the nucleus. The induced Skp2/Cks1 degrades p27 in tubular epithelial cells in UUO kidneys, allowing tubular epithelial cell proliferation to increase [76]. Tubular dilation occurs as a result of the increase in the tubular epithelial cell number and ultimately leads to progressive nephropathy [26]

Cks1

Cks1 is an essential cofactor for ligation of ubiquitin to p27. It recognizes Thr187-phosphorylated p27 and is essential for the rigid binding between p27 and Skp2 that results in Skp2-mediated degradation of p27 [9, 10]. We previously reported that the mRNA and protein levels of Cks1 are increased in the early stages of renal damage [76]. Cks1 protein is mainly localized in the nuclei and to a lesser extent in the cytoplasm of tubular epithelial cells. Similar to Skp2, Cks1 colocalizes with RelB in the nuclei of tubular epithelial cells. These results suggest that Skp2 and Cks1 collaboratively promote p27 degradation via the ubiquitin proteasome pathway and induce tubular epithelial cell proliferation in the early stages of renal damage, resulting in tubular dilation in chronic nephropathy. The mRNA level of Cks1 is also significantly upregulated in TNF-α-stimulated NRK cells. We also reported that a sequence (GGGACTTCC) in the rodent Cks1 promoter is similar to the putative NF-κB element (GGGACTTTCC) at nine of the ten nucleotides. Therefore, it is seems likely that the TNF-α/NF-κB signaling pathway promotes the transcription of both Skp2 and Cks1 in renal injury [76].

p27

The CKI p27 is an important regulator of cell proliferation that negatively regulates the behavior of CDKs in the cell cycle [81, 82]. p27 is abundantly expressed in most normal quiescent cells, but its level decreases during progression to the S phase in response to a proliferative/mitotic stimulus [3, 4]. In vitro studies have shown that an experimental decrease of p27 protein enhances the proliferative response to mitogens [83, 84], while forced overexpression of p27 protein inhibits cell proliferation [4]. Additionally, p27 is destabilized in many types of human cancer, which is implicated in the aggressiveness and poor prognosis of tumors [77, 85–87]. The protein level of p27 is controlled transcriptionally and by proteolytic degradation of p27 protein via the ubiquitin-proteasome pathway. p27 is phosphorylated on Thr187 by CDK [9, 10], and Thr187-phosphorylated p27 is a specific target for the SCF/Skp2/Cks1 complex to induce its ubiquitin-dependent degradation [9, 11]. This is consistent with observations that Skp2-deficient mice and/or

Cks1-deficient mice exhibit cellular accumulation of p27 and a small body size compared with wild-type mice [9, 10].

In normal kidneys, p27 is expressed in most tubular epithelial cells to maintain their quiescent status. The level of p27 protein decreases rapidly in UUO kidneys, allowing proliferation of tubular epithelial cells and tubule dilation in the early stages of nephropathy. The mRNA and protein levels of p27 are subsequently upregulated in UUO mice [88, 89]. It was reported that renal tubular epithelial cell proliferation and apoptosis are markedly increased in the obstructed kidney of $p27^{-/-}$ mice [90]. Additionally, the magnitude of p27 protein upregulation in obstructed kidneys is greater in $Skp2^{-/-}$ mice than in $Skp2^{+/+}$ mice. In the UUO kidneys of $Skp2^{-/-}$ mice, tubular epithelial cell proliferation is inhibited by the accumulation of p27, preventing an increase in tubular epithelial cell number. Furthermore, apoptosis and tubulointerstitial fibrosis are markedly attenuated in the obstructed kidneys of $Skp2^{-/-}$ mice [20]. It is well known that renal fibroblast activation and proliferation are involved in the progression of chronic kidney disease [19]. We also reported that UUO stimulates renal interstitial cell proliferation and significantly increased the number of interstitial cells in the UUO kidney [20]. The enhanced interstitial cell proliferation and the increase in number of α-SMA-positive myofibroblasts were partially inhibited by Skp2-deficiency. p21 is the critical negative regulator of interstitial fibroblast proliferation [91]. We have shown that p21 accumulation in UUO kidneys is moderately enhanced by Skp2 deficiency [20]. In addition, the accumulation of p21 and p27 as a result of proteasome inhibition is associated with inhibition of interstitial fibroblast proliferation [92]. Therefore, p21 and p27 are negative regulators of interstitial cell proliferation while upregulated Skp2 in the UUO kidney enhances their degradation to promote interstitial fibroblast proliferation and myofibroblast formation as critical stages in the EMT. Taken together, these results suggest that Skp2 has important roles in the control of p27 and p21 in the kidney. In addition, Skp2, as induced by renal damage, promotes the proliferation of tubular epithelial cells and interstitial fibroblasts by enhancing the degradation of p27 and p21. Although further investigation is required to determine whether renal function was recovered by Skp2 deficiency, the histopathological features of $Skp2^{-/-}$ UUO kidney were apparently improved compared with the WT UUO kidney. Many other studies have demonstrated increased p27 expression in other models of renal disease, including diabetic nephropathy [30, 31] and cisplatin-induced acute renal failure [93]. In kidney cells, mesangial cells (MC) play a key role in glomerular hypertrophy in early diabetic nephropathy [94] by secreting extracellular matrix proteins that contribute to the development of glomerulosclerosis. Increased p27 expression in the glomerulus causes proliferation arrest and hypertrophy of MCs during early diabetic nephropathy. p27 is also highly expressed in the normal quiescent rat glomeruli, but its expression decreases in proliferating MCs in the ATS model of nephropathy [95]. The p27 expression level returns to the basal level after the resolution of MC proliferation [96]. Podocyte proliferation is also markedly increased in association with glomerulonephritis in $p27^{-/-}$ mice [97]. These data indicate that p27 regulates the proliferation of various types of renal cells, and its upregulation stops excessive renal cell proliferation to protect cells and tissues from inflammatory injury.

Renal damages in $Skp2^{-/-}p27^{-/-}$ mice

Unlike the marked amelioration of renal injury associates with renal accumulation of p27 in tubular epithelial cells in $Skp2^{-/-}$ mice, $Skp2^{-/-}/p27^{-/-}$ double knockout mice show marked progression of tubular dilatation as a result of the enhanced tubular epithelial cell proliferation that occurs through the loss of p27 [97]. Notably, the tubular epithelial cell number in UUO kidneys is much greater in $Skp2^{-/-}p27^{-/-}$ mice than in wild-type mice. Furthermore, interstitial cell proliferation in UUO kidneys is also greater in $Skp2^{-/-}p27^{-/-}$ mice than in $Skp2^{-/-}$ mice. The expression levels of vimentin, α-SMA, type I collagen, and fibronectin, components of the extracellular matrix, are significantly decreased in the UUO kidneys of $Skp2^{-/-}$ mice. While extracellular matrix production and macrophage infiltration are more pronounced in these mice, tubulointerstitial fibrosis progresses more in $Skp2^{-/-}p27^{-/-}$ mice compared with $Skp2^{-/-}$ mice [20, 91]. These results suggest that Skp2 may regulate extracellular matrix synthesis by modulating p27 expression/activity in renal diseases. Taken together, these results indicate that the ameliorative effects of Skp2 deficiency following UUO are canceled by p27 deficiency in $Skp2^{-/-}p27^{-/-}$ mice. As described above, it has been reported that proliferation is inhibited, and that the expression of p21 and p27 is increased by proteasome inhibitors in two nasal fibroblast cell lines. In these cell lines, treatment with a proteasome inhibitor suppressed fibrosis together with reduced MCP-1 production and TGF-β- and TNF-α-induced collagen mRNA expression. Moreover, the inflammatory response in fibroblasts is inhibited by suppression of IL-1β-/TNF-α-induced NF-κB activation and IL-1β-induced IL-6/8 production [92]. These results suggest that the accumulated p21 and p27 in fibroblasts can inhibit tissue inflammation and progressive fibrosis. In the UUO kidneys of $Skp2^{-/-}$ mice, extracellular matrix production, inflammation, and renal fibrosis may be ameliorated by p27 accumulation.

In addition to p27, Skp2 targets several other proteins that control the cell cycle, including p21, p57, cyclin E, cyclin A, and cyclin D1, for degradation via the ubiquitin-dependent proteasome pathway. Interestingly, the protein

levels of other Skp2 targets, including p57, p130, TOB1, cyclin A, and cyclin D1, in UUO kidneys were not significantly increased in Skp2$^{-/-}$ mice compared with wild-type mice. Although the levels of p21, c-Myc, b-Myb, and cyclin E, in the UUO kidneys were slightly increased in Skp2$^{-/-}$ mice, the magnitudes of the increments did not reflect the accumulation of p27 [97]. These findings suggest that p27 is the main target of Skp2 and that the reduction in p27 levels has a pathogenic role in the progression of nephropathy.

Other cell cycle regulators involved in nephropathy

p21

The CKI protein p21 has important roles in controlling cell proliferation, terminal differentiation, cellular senescence, and apoptosis [81]. p21 inhibits the cell cycle progression by binding to cyclin/CDK complexes. p21 also directly binds to proliferating cell nuclear antigen (PCNA), which inhibits the involvement of PCNA in DNA replication [98, 99]. The protein level of p21 increases in Skp2$^{-/-}$ mouse embryo fibroblasts during the S-phase, and its degradation is low in Skp2$^{-/-}$ cells, which suggests that p21 is a target of Skp2 degradation in the S-phase [100]. The p21 protein level is mainly controlled by transcription, but it is also subject to ubiquitin-independent and -dependent degradation [101]. In the kidneys, p21 is upregulated in the early stages of renal injury in UUO mice [102] and ATS nephropathy [95], as well as in ischemia [103] and cisplatin-treated mice [104]. p21 levels increase dramatically following growth arrest induced by the tumor suppressor protein p53 and in the early stage of differentiation [81, 105]. p21 is also induced in p53-mediated apoptosis, as the p53-dependent pathways are involved in transactivation of the p21 gene [106]. However, p21 mRNA expression was enhanced in p53-deficient mice with nephropathy, which suggests that p21 transcriptional activation occurs via a p53-independent pathway in renal damage [104]. Huge et al. also reported that the proliferation of interstitial cells, particularly myofibroblasts, was promoted in the UUO kidneys from p21$^{-/-}$ mice compared with wild-type mice resulting in progression of renal failure, although there was no difference in the rate of interstitial cell apoptosis between these two strains. Tubular epithelial cell proliferation and apoptosis were also unchanged in the obstructed kidney from p21$^{-/-}$ mice [91]. p21 plays a limited role in the proliferation of myofibroblasts in renal damage, and is not essential for the regulation of tubular epithelial cell proliferation or apoptosis following UUO. However, it was reported that p21 expression is increased in experimental diabetic nephropathy and inhibits mesangial cell proliferation [107]. Moreover, glomerular cell proliferation is significantly increased in glomerulonephritis in p21$^{-/-}$ mice [108]. Taken together, these results indicate that p21 regulates the proliferation of myofibroblasts and glomerular cells in nephropathy.

p57

The CKI protein p57 inhibits cell cycle progression into the S-phase. Overexpression of p57 induces G1-phase arrest [109, 110] and is implicated in cell cycle exit accompanying terminal differentiation [111, 112]. p57 is constitutively expressed in terminally differentiated normal mature podocytes [113, 114]. In glomerular diseases, p57 expression is decreased in podocytes, allowing mature podocytes to proliferate and acquire an immature phenotype in response to renal injury. In the ATS model, which is associated with podocyte injury, p57 expression is markedly decreased in proliferating podocytes [115]. However, the p57 protein level remains unchanged during differentiation in cultured podocytes. These properties suggest that p57 controls the proliferation of mature podocytes in nephropathy.

p53

p53 is associated with cell proliferation, DNA repair, maintenance of DNA integrity, and apoptosis [116]. p53 regulates the induction of p21 and growth-arrested DNA damage protein 45 (GADD45) to control cell replication [117, 118]. p53 mRNA expression increases rapidly after UUO. p53 induces apoptosis of severely damaged tubular cells to limit renal damage [102]. However, tubular apoptosis after UUO is also mediated by p53-independent pathways [119].

Perspectives

The number of patients with end-stage renal disease requiring renal replacement therapy is steadily increasing worldwide. However, the most effective therapies for this devastating disease are dialysis or kidney transplantation. Therefore, it is important to develop novel molecular targets for chronic kidney disease and avoid its progression to end-stage renal disease. Considering the results of that reports described above, it seems likely that proteasome inhibitors have some effects on Skp2-dependent protein degradation and may offer a new therapeutic drug for nephropathy, such as kidney obstruction. It has been reported that renal fibrosis is ameliorated by proteasome inhibitors in rat obstructive nephropathy [120]. Therefore, Neubert et al. [121] suggested that proteasome inhibitors are effective for treatment of nephropathy, and Pujols et al. [92] reported that a proteasome inhibitor could reduce proliferation, collagen production, and inflammatory responses in nasal fibroblasts.

However, proteasome inhibitors reportedly show severe side effects because they accumulate many proteins by inhibition of proteasome-mediated degradation [22]. A described above, renal damage in UUO kidneys, including interstitial fibrosis, is markedly attenuated in Skp2$^{-/-}$ mice compared with wild-type mice. The decreased tubular epithelial cell proliferation and reduced tubule dilation may effect the inhibition of EMT [22, 34–36] in the UUO kidneys of Skp2$^{-/-}$ mice. We suggest that the progression of renal damage is stopped at an early stage by Skp2 deletion, reducing the extent of renal fibrosis in UUO kidneys of Skp2$^{-/-}$ mice. Cks1 also increases p27 degradation in the early stage of renal damage, and Skp2 and Cks1 promote p27 degradation selectively in a collaborative manner. Therefore, we think an inhibitor for SCF-Skp2/Cks1 E3 ligase will offer a specific therapeutic target for renal injury and is likely to inhibit the progression of nephropathy.

References

1. Morgan DO (1995) Principles of CDK regulation. Nature 374:131–134
2. Sherr CJ, Roberts JM (1995) Inhibitors of mammalian G1 cyclin-dependent kinases. Genes Dev 9:1149–1163
3. Nourse J, Firpo E, Flanagan WM et al (1994) Interlukin-2-mediated elimination of the p27kip1 cyclin-dependent kinases inhibitor prevented by rapamycin. Nature 372:570–573
4. Polyak K, Lee MH, Erdjument-Bromage H et al (1994) Cloning of p27kip1, a cyclin-dependent kinases inhibitor and potential mediator of extracellular antimitogenic signals. Cell 78:59–66
5. Weissman AM (1997) Regulating protein degradation by ubiquitination. Immunol Today 18:189–198
6. Hershko A, Ciechanover A (1998) The ubiquitin system. Annu Rev Biochem 67:425–479
7. Carrano AC, Eytan E, Hershko A et al (1999) SKP2 is required for ubiquitin-mediated degradation of the CDK inhibitor p27. Nat Cell Biol 1:193–199
8. Tsvetkov LM, Yeh KH, Lee SJ et al (1999) p27(Kip1) ubiquitination and degradation is regulated by the SCF(Skp2) complex through phosphorylated Thr187 in p27. Curr Biol 9:661–664
9. Spruck C, Strohmaier H, Watson M et al (2001) A CDK-independent function of mammalian Cks1: targeting of SCF (Skp2) to the CDK inhibitor p27Kip1. Mol Cell 7:639–650
10. Ganoth D, Bornstein G, Ko TK et al (2001) The cell-cycle regulatory protein Cks1 is required for SCF-Skp2-mediated ubiquitinylation of p27. Nat Cell Biol 3:321–324
11. Nakayama K, Nagahama H, Minamishima YA et al (2000) Targeted disruption of Skp2 results in accumulation of cyclin E and p27kip1, polyploidy and centrosome overduplication. EMBO J 19(9):2069–2081
12. Couser WG, Johnson RJ (1994) Mechanisms of progressive renal disease in glomerulonephritis. Am J Kidney Dis 23:193–198
13. Gobe GC, Axelsen RA (1987) Genesis of renal tubular atrophy in experimental hydronephrosis in the rat. Role of apoptosis. Lab Invest 56:273–281
14. Walton G, Buttyan R, Garcia Montes E et al (1992) Renal growth factor expression during the early phase of experimental hydronephrosis. J Urol 148:510–514
15. Klahr S, Morrissey J (2002) Obstructive nephropathy and renal fibrosis. Am J Physiol Renal Physiol 283:F861–F875
16. Fukasawa H, Yamamoto T, Togawa A et al (2006) Ubiquitin-dependent degradation of SnoN and Ski is increased in renal fibrosis induced by obstructive injury. Kidney Int 69:1733–1740
17. Schreiner GF, Harris KP, Purkerson ML et al (1988) Immunological aspects of acute ureteral obstruction: immune cell infiltrate in the kidney. Kidney Int 34(4):487–493
18. Ricardo SD, Levinson ME, DeJoseph MR et al (1996) Expression of adhesion molecules in rat renal cortex during experimental hydronephrosis. Kidney Int 50(6):2002–2010
19. Chevalier RL, Forbes MS, Thornhill BA et al (2009) Ureteral obstruction as a model of renal interstitial fibrosis and obstructive nephropathy. Kidney Int 75:1145–1152
20. Suzuki S, Fukasawa H, Kitagawa K et al (2007) Renal damage in obstructive nephropathy is decreased in Skp2-deficient mice. Am J Pathol 171(2):473–483
21. Misaki T, Yamamoto T, Suzuki S et al (2009) Decrease in tumor necrosis factor-alpha receptor-associated death domain results from ubiquitin-dependent degradation in obstructive renal injury in rats. Am J Pathol 175(1):74–83
22. Yamashita S, Maeshima A, Nojima Y (2005) Involvement of renal progenitor tubular cells in epithelial-to-mesenchymal transition in fibrotic rat kidneys. J Am Soc Nephrol 16(7):2044–2051
23. Liu Y (2004) Epithelial to mesenchymal transition in renal fibrogenesis: pathologic significance, molecular mechanism, and therapeutic intervention. J Am Soc Nephrol 15(1):1–12
24. Fukasawa H, Fujigaki Y, Yamamato T et al (2012) Protein degradation by the ubiquitin-proteasome pathway and organ fibrosis. Curr Med Chem 19:893–900
25. Yamamoto T, Noble NA, Miller DE et al (1994) Sustained expression of TGF-beta1 underlies development of progressive kidney fibrosis. Kidney Int 45:916–927
26. Watanabe T, Yamamoto T, Ikegaya N et al (2002) Transforming growth factor-beta receptors in self-limited vs. chronic progressive nephropathy in rats. J Pathol 198(3):397–406
27. Fukasawa H, Yamamoto T, Suzuki H et al (2004) Treatment with anti-TGF-beta antibody ameliorates chronic progressive nephritis by inhibiting Smad/TGF-beta signaling. Kidney Int 65:63–74
28. Ng YY, Huang TP, Yang WC (1998) Tubular epithelial-myofibroblast transdifferentiation in progressive tubulointerstitial fibrosis in 5/6 nephrectomized rats. Kidney Int 54(3):864–876
29. Sinuani I, Weissgarten J, Beberashvili I et al (2009) The cyclin kinase inhibitor p57kip2 regulates TGF-beta-induced compensatory tubular hypertrophy: effect of the immunomodulator AS101. Nephrol Dial Transplant 24(8):2328–3238
30. Wolf G, Schroeder R, Thaiss F et al (1998) Glomerular expression of p27Kip1 in diabetic db/db mouse: role of hyperglycemia. Kidney Int 53(4):869–879
31. Awazu M, Omori S, Ishikura K et al (2003) The lack of cyclin kinase inhibitor p27(Kip1) ameliorates progression of diabetic nephropathy. J Am Soc Nephrol 14(3):699–708
32. Border WA, Ruoslahti E (1992) Transforming growth factor-beta in disease: the dark side of tissue repair. J Clin Invest 90:1–7
33. Eddy AA (1996) Molecular insights into renal interstitial fibrosis. J Am Soc Nephrol 7:2495–2508
34. Border WA, Noble NA (1994) Transforming growth factor beta in tissue fibrosis. N Engl J Med 331:1286–1292
35. Okada H, Danoff TM, Kalluri R et al (1997) Early role of Fsp1 in epithelial-mesenchymal transformation. Am J Physiol 273:F563–F574

36. Fan JM, Ng YY, Hill PA et al (1999) Transforming growth factor-beta regulates tubular epithelial-myofibroblast transdifferentiation in vitro. Kidney Int 56:1455–1467
37. Robert LC (2006) Obstructive nephropathy: towards biomarker discovery and gene therapy. Nat Clin Pract Nephrol 2:157–168
38. García-Sánchez O, López-Hernández FJ, López-Novoa JM (2010) An integrative view on the role of TGF-beta in the progressive tubular deletion associated with chronic kidney disease. Kidney Int 77(11):950–955
39. Yu L, Hébert MC, Zhang YE (2002) TGF-beta receptor-activated p38 MAP kinase mediates Smad-independent TGF-beta responses. EMBO J 21(14):3749–3759
40. Dai C, Yang J, Liu Y (2003) Transforming growth factor-beta1 potentiates renal tubular epithelial cell death by a mechanism independent of Smad signaling. J Biol Chem 278(14):12537–12545
41. Ohashi N, Yamamoto T, Uchida C et al (2005) Transcriptional induction of Smurf2 ubiquitin ligase by TGF-β. FEBS Lett 579:2557–2563
42. Fukasawa H, Yamamato T, Kitagawa M et al (2008) Regulation of TGF-beta signaling by Smads and its roles in tissue fibrosis. Curr Signal Trunsduct Ther 3:1–6
43. Böttinger EP, Bitzer M (2002) TGF-beta signaling in renal disease. J Am Soc Nephrol 13:2600–2610
44. Lin H, Wang D, Wu T et al (2011) Blocking core fucosylation of TGF-β1 receptors downregulates their functions and attenuates the epithelial-mesenchymal transition of renal tubular cells. Am J Physiol Renal Physiol 300:F1017–F1025
45. Derynck R, Zhang Y, Feng XH (1998) Smads: transcriptional activators of TGF-beta responses. Cell 95(6):737–740
46. Togawa A, Yamamoto T, Suzuki H et al (2003) Ubiquitin-dependent degradation of Smad2 is increased in the glomeruli of rats with anti-thymocyte serum nephritis. Am J Pathol 163(4):1645–1652
47. Wang W, Koka V, Lan HY (2005) Transforming growth factor-beta and Smad signalling in kidney diseases. Nephrology 10(1):48–56
48. Fukasawa H, Yamamoto T, Togawa A et al (2004) Down-regulation of Smad7 expression by ubiquitin-dependent degradation contributes to renal fibrosis in obstructive nephropathy in mice. Proc Natl Acad Sci USA 101(23):8687–8692
49. Oh SP, Seki T, Goss KA et al (2000) Activin receptor-like kinase 1 modulates transforming growth factor-beta 1 signaling in the regulation of angiogenesis. PNAS 97:2626–2631
50. Wang W, Ungermannova D, Jin J et al (2004) Negative regulation of SCFSkp2 ubiquitin ligase by TGF-beta signaling. Oncogene 23(5):1064–1075
51. Liu W, Wu G, Li W et al (2007) Cdh1-anaphase-promoting complex targets Skp2 for destruction in transforming growth factor beta-induced growth inhibition. MCB 27(8):2967–2979
52. Hu D, Liu W, Wu G et al (2011) Nuclear translocation of Skp2 facilitates its destruction in response to TGFβ signaling. Cell Cycle 10(2):285–292
53. He KL, Ting AT (2002) A20 inhibits tumor necrosis factor (TNF) alpha-induced apoptosis by disrupting recruitment of TRADD and RIP to the TNF receptor 1 complex in Jurkat T cells. Mol Cell Biol 22:6034–6045
54. Misseri R, Meldrum DR, Dinarello CA et al (2005) TNF-alpha mediates obstruction-induced renal tubular cell apoptosis and proapoptotic signaling. Am J Physiol Renal Physiol 288:F406–F411
55. Meldrum KK, Metcalfe P, Leslie JA et al (2006) TNF-alpha neutralization decreases nuclear factor-kappaB activation and apoptosis during renal obstruction. J Surg Res 13:182–188
56. Meldrum KK, Misseri R, Metcalfe P et al (2007) TNF-alpha neutralization ameliorates obstruction-induced renal fibrosis. Am J Physiol Regul Integr Comp Physiol 292:1456–1464
57. Ramesh G, Reeves WB (2003) TNFR2-mediated apoptosis and necrosis in cisplatin-induced acute renal failure. Am J Physiol Renal Physiol 285:F610–F618
58. Bharat BA (2003) Signaling pathways of the superfamily: a double-edged sword. Immunology 3:745–756
59. Gioacchino N, Liv MIA (2008) A birthday gift for TRADD. Nat Immunol 9(9):1015–1016
60. Wang D, Montgomery RB, Schmidt LJ et al (2009) Reduced tumor necrosis factor receptor-associated death domain expression is associated with prostate cancer progression. Cancer Res 69(24):9448–9456
61. Hsu H, Shu HB, Pan MG et al (1996) TRADD-TRAF2 and TRADD-FADD interactions define two distinct TNF receptor 1 signal transduction pathways. Cell 84:299–308
62. Rothe M, Sarma V, Dixit VM et al (1995) TRAF2-mediated activation of NF-kappa B by TNF receptor 2 and CD40. Science 269:1424–1427
63. Guo G, Morrissey J, McCracken R et al (1999) Role of TNFR1 and TNFR2 receptors in tubulointerstitial fibrosis of obstructive nephropathy. Am J Physiol 277:F766–F772
64. Weiss T, Grell M, Siemienski K et al (1998) TNFR80-dependent enhancement of TNFR60-induced cell death is mediated by TNFR-associated factor 2 and is specific for TNFR60. J Immunol 161(6):3136–3142
65. Mukhopadhyay A, Suttles J, Stout RD et al (2001) Genetic deletion of the tumor necrosis factor receptor p60 or p80 abrogates ligand-mediated activation of nuclear factor-kappa B and of mitogen-activated protein kinases in macrophages. J Biol Chem 276(34):31906–31912
66. Collins T (1993) Endothelial nuclear factor-kappa B and the initiation of the atherosclerotic lesion. Lab Invest 68(5):499–508
67. Baeuerle PA, Henkel T (1994) Function and activation of NF-kappa B in the immune system. Annu Rev Immunol 12:141–179
68. Tak PP, Firestein GS (2001) NF-κB: a key role in inflammatory disease. J Clin Invest 107:7–11
69. Ruiz-Ortega M, Bustos C, Hernández-Presa MA (1998) Angiotensin II participates in mononuclear cell recruitment in experimental immune complex nephritis through nuclear factor-kappa B activation and monocyte chemoattractant protein-1 synthesis. J Immunol 161(1):430–439
70. Pocock J, Gómez-Guerrer C, Harendza S et al (2003) Differential activation of NF-κB, AP-1, and C/EBP in endotoxin-tolerant rats: mechanisms for in vivo regulation of glomerular RANTES/CCL5 expression. J Immunol 170(12):6280–6291
71. Hayden MS, Ghosh S (2004) Signaling to NF-kappaB. Genes Dev 1:2195–2224
72. Cao Y, Bonizzi G, Seagroves TN et al (2001) IKKalpha provides an essential link between RANK signaling and cyclin D1 expression during mammary gland development. Cell 107:763–775
73. Morrissey JJ, Klahr S (1997) Rapid communication. Enalapril decreases nuclear factor kappa B activation in the kidney with ureteral obstruction. Kidney Int 52(4):926–933
74. Schneider G, Saur D, Siveke JT et al (2006) IKK alpha controls p52/RelB at the skp2 gene promoter to regulate G1- to S-phase progression. EMBO J 25:3801–3812
75. Barré B, Perkins ND (2010) The Skp2 promoter integrates signaling through the NF-kappaB, p53, and Akt/GSK3beta pathways to regulate autophagy and apoptosis. Mol Cell 38:524–538
76. Suzuki S, Fukasawa H, Misaki T et al (2011) Up-regulation of Cks1 and Skp2 with TNFα/NF-κB signaling in chronic progressive nephropathy. Genes Cells 16(11):1110–1120
77. Frescas D, Pagano M (2008) Deregulated proteolysis by the F-box proteins SKP2 and beta-TrCP: tipping the scales of cancer. Nat Rev Cancer 8:438–449

78. Sutterlüty H, Chatelain E, Marti A et al (1999) p45SKP2 promotes p27Kip1 degradation and induces S phase in quiescent cells. Nat Cell Biol 1:207–214
79. Kamura T, Hara T, Matsumoto M et al (2004) Cytoplasmic ubiquitin ligase KPC regulates proteolysis of p27(Kip1) at G1 phase. Nat Cell Biol 6:1229–1235
80. Hattori T, Isobe T, Abe K et al (2007) Pirh2 Promotes Ubiquitin-Dependent Degradation of the CDK Inhibitor $p27^{Kip1}$. Cancer Res 67:10789–10795
81. Sherr CJ, Roberts JM (1999) CDK inhibitors: positive and negative regulators of G1-phase progression. Genes Dev 13(12):1501–1512
82. Elledge SJ, Winston J, Harper JW (1996) A question of balance: the role of cyclin-kinase inhibitors in development and tumorigenesis. Trends Cell Biol 6(10):388–392
83. Coats S, Flanagan WM, Nourse J et al (1996) Requirement of $p27^{kipl}$ for restriction point control of the fibroblast cell cycle. Science 272:877–880
84. Shankland SJ, Pippin J, Flanagan M et al (1997) Mesangial cell proliferation mediated by PDGF and bFGF is determined by levels of the cyclin kinase inhibitor $p27^{kipl}$. Kidney Int 51:1088–1099
85. Loda M, Cukor B, Tam SW et al (1997) Increased proteasome-dependent degradation of the cyclin-dependent kinase inhibitor p27 in aggressive colorectal carcinomas. Nat Med 3(2):231–234
86. Esposito V, Baldi A, De Luca A et al (1997) Prognostic role of the cyclin-dependent kinase inhibitor p27 in non-small cell lung cancer. Cancer Res 57(16):3381–3385
87. Steeg PS, Abrams JS (1997) Cancer prognostics: past, present and p27. Nat Med 3(2):152–154
88. Gerth JH, Kriegsmann J, Trinh TT et al (2002) Induction of $p27^{KIP1}$ after unilateral ureteral obstruction is independent of angiotensin II. Kidney Int 61:68–79
89. Schaefer L, Macakova K, Raslik L et al (2002) Absence of decorin adversely influences tubulointerstitial fibrosis of the obstructed kidney by enhanced apoptosis and increased inflammatory reaction. Am J Pathol 160(3):1181–1191
90. Ophascharoensuk V, Fero ML, Hughes J et al (1998) The cyclin-dependent kinases inhibitor $p27^{kipl}$ safeguards against inflammatory injury. Nat Med 4:575–580
91. Hughes J, Brown P, Shankland SJ (1999) Cyclin kinase inhibitor p21CIP1/WAF1 limits interstitial cell proliferation following ureteric obstruction. Am J Physiol 277:F948–F956
92. Pujols L, Fernández-Bertolín L, Fuentes-Prado M et al (2012) Proteasome inhibition reduces proliferation, collagen expression, and inflammatory cytokine production in nasal mucosa and polyp fibroblasts. J Pharmacol Exp Ther 343(1):184–197
93. Zhou H, Kato A, Yasuda H et al (2004) The induction of cell cycle regulatory and DNA repair proteins in cisplatin-induced acute renal failure. Toxicol Appl Pharmacol 200(2):111–120
94. Ibrahim HN, Hostetter TH (1997) Diabetic nephropathy. J Am Soc Nephrol 8(3):487–493
95. Chiara M, Menegatti E, Di Simone D et al (2004) Mycophenolate mofetil and roscovitine decrease cyclin expression and increase p27(kip1) expression in anti Thy1 mesangial proliferative nephritis. Clin Exp Immunol 139(2):225–235
96. Shankland SJ, Hugo C, Coats SR (1996) Changes in cell-cycle protein expression during experimental mesangial proliferative glomerulonephritis. Kidney Int 50(4):1230–1239
97. Suzuki S, Fukasawa H, Misaki T et al (2012) The amelioration of renal damage in Skp2-deficient mice canceled by p27 Kip1 deficiency in $Skp2^{-/-}$ $p27^{-/-}$ mice. PLoS One 7(4):e36249
98. Li R, Waga S, Hannon GJ et al (1994) Differential effects by the p21 CDK inhibitor on PCNA-dependent DNA replication and repair. Nature 371:534–537
99. Chen J, Jackson PK, Kirschner MW et al (1995) Separate domains of p21 involved in the inhibition of Cdk kinase and PCNA. Nature 374:386–388
100. Bornstein G, Bloom J, Sitry-Shevah D et al (2003) Role of the SCFSkp2 ubiquitin ligase in the degradation of p21Cip1 in S phase. J Biol Chem 278(28):25752–25757
101. Sheaff RJ, Singer JD, Swanger J et al (2000) Proteasomal turnover of p21Cip1 does not require p21Cip1 ubiquitination. Mol Cell 5(2):403–410
102. Morrissey JJ, Ishidoya S, McCrachen R et al (1996) Control of p53 and p21 (WAF1) expression during unilateral ureteral obstruction. Kidney Int Suppl 57:S84–S92
103. Megyesi J, Udvarhelyi N, Safirstein RL et al (1996) The p53-independent activation of transcription of p21 WAF1/CIP1/SDI1 after acute renal failure. Am J Physiol 271:F1211–F1216
104. Zhou H, Fujigaki Y, Kato A et al (2006) Inhibition of p21 modifies the response of cortical proximal tubules to cisplatin in rats. Am J Physiol Renal Physiol 291(1):F225–F235
105. Waga S, Hannon GJ, Beach D et al (1994) The p21 inhibitor of cyclin-dependent kinases controls DNA replication by interaction with PCNA. Nature 369:574–578
106. El-Deiry WS, Harper JW, O'Connor PM et al (1994) WAF1/CIP1 is induced in p53-mediated G_1 arrest and apoptosis. Cancer Res 54(5):1169–1174
107. Kuan CJ, al-Douahji M, Shankland SJ (1998) The cyclin kinase inhibitor p21WAF1, CIP1 is increased in experimental diabetic nephropathy: potential role in glomerular hypertrophy. J Am Soc Nephrol 9(6):986–993
108. Kim YG, Alpers CE, Brugarolas J et al (1999) The cyclin kinase inhibitor p21CIP1/WAF1 limits glomerular epithelial cell proliferation in experimental glomerulonephritis. Kidney Int 55(6):2349–2361
109. Lee MH, Reynisdóttir I, Massagué J (1995) Cloning of p57KIP2, a cyclin-dependent kinase inhibitor with unique domain structure and tissue distribution. Genes Dev 9(6):639–649
110. Matsuoka S, Edwards MC, Bai C et al (1995) p57KIP2, a structurally distinct member of the p21CIP1 Cdk inhibitor family, is a candidate tumor suppressor gene. Genes Dev 9(6):650–662
111. Zhang P, Wong C, DePinho RA (1998) Cooperation between the Cdk inhibitors p27(KIP1) and p57(KIP2) in the control of tissue growth and development. Genes Dev 12(20):3162–3167
112. Lovicu FJ, McAvoy JW (1999) Spatial and temporal expression of p57(KIP2) during murine lens development. Mech Dev 86(1–2):165–169
113. Nagata M, Nakayama K, Terada Y et al (1998) Cell cycle regulation and differentiation in the human podocyte lineage. Am J Pathol 153(5):1511–1520
114. Shankland SJ, Eitner F, Hudkins KL et al (2000) Differential expression of cyclin-dependent kinase inhibitors in human glomerular disease: role in podocyte proliferation and maturation. Kidney Int 58(2):674–683
115. Hiromura K, Haseley LA, Zhang P et al (2001) Podocyte expression of the CDK-inhibitor p57 during development and disease. Kidney Int 60(6):2235–2246
116. Hartwell LH, Kastan MB (1994) Cell cycle control and cancer. Science 266:1821–1828
117. El-Deiry WS, Tokino T, Velculescu VE et al (1993) WAF1, a potential mediator of p53 tumor suppression. Cell 75(4): 817–825
118. Smith ML, Chen IT, Zhan Q et al (1994) Interaction of the p53-regulated protein Gadd45 with proliferating cell nuclear antigen. Science 266:1376–1380
119. Choi YJ, Mendoza L, Rha SJ et al (2001) Role of p53-dependent activation of caspases in chronic obstructive uropathy: evidence from p53 null mutant mice. J Am Soc Nephrol 12(5):983–992

120. Tashiro K, Tamada S, Kuwabara N et al (2003) Attenuation of renal fibrosis by proteasome inhibition in rat obstructive nephropathy: possible role of nuclear factor kappaB. Int J Mol Med 12:587–592
121. Neubert K, Meister S, Moser K et al (2008) The proteasome inhibitor bortezomib depletes plasma cells and protects mice with lupus-like disease from nephritis. Nat Med 14:748–755
122. Huber JM, Tagwerker A, Heininger D et al (2009) The proteasome inhibitor bortezomib aggravates renal ischemia-reperfusion injury. Am J Physiol Renal Physiol 297: F451–F460

The EMBO Journal (2012) 31, 2365–2377 | © 2012 European Molecular Biology Organization | All Rights Reserved 0261-4189/12
www.embojournal.org

THE EMBO JOURNAL

Chk1 phosphorylates the tumour suppressor Mig-6, regulating the activation of EGF signalling

Ning Liu[1,2], Masaki Matsumoto[3], Kyoko Kitagawa[1], Yojiro Kotake[1], Sayuri Suzuki[1], Senji Shirasawa[4], Keiichi I Nakayama[3], Makoto Nakanishi[5], Hiroyuki Niida[1] and Masatoshi Kitagawa[1,*]

[1]Department of Molecular Biology, Hamamatsu University School of Medicine, Hamamatsu, Shizuoka, Japan, [2]Department of Infectious Diseases, Shengjing Hospital of China Medical University, Shenyang, China, [3]Department of Molecular and Cellular Biology, Medical Institute of Bioregulation, Kyushu University, Higashi-ku, Fukuoka, Japan, [4]Department of Cell Biology, Faculty of Medicine, Fukuoka University, Jonan-ku, Fukuoka, Japan and [5]Department of Biochemistry, Nagoya City University Medical School, Mizuho-ku, Nagoya, Japan

The tumour suppressor gene product Mig-6 acts as an inhibitor of epidermal growth factor (EGF) signalling. However, its posttranslational modifications and regulatory mechanisms have not been elucidated. Here, we investigated the phosphorylation of human Mig-6 and found that Chk1 phosphorylated Mig-6 *in vivo* as well as *in vitro*. Moreover, EGF stimulation promoted phosphorylation of Mig-6 without DNA damage and the phosphorylation was inhibited by depletion of Chk1. EGF also increased Ser280-phosphorylated Chk1, a cytoplasmic-tethering form, via PI3K pathway. Mass spectrometric analyses suggested that Ser 251 of Mig-6 was a major phosphorylation site by Chk1 *in vitro* and *in vivo*. Substitution of Ser 251 to alanine increased inhibitory activity of Mig-6 against EGF receptor (EGFR) activation. Moreover, EGF-dependent activation of EGFR and cell growth were inhibited by Chk1 depletion, and were rescued by co-depletion of Mig-6. Our results suggest that Chk1 phosphorylates Mig-6 on Ser 251, resulting in the inhibition of Mig-6, and that Chk1 acts as a positive regulator of EGF signalling. This is a novel function of Chk1.

The EMBO Journal (2012) **31**, 2365–2377. doi:10.1038/emboj.2012.88; Published online 13 April 2012
Subject Categories: signal transduction; molecular biology of disease
Keywords: Chk1; EGFR; Mig-6; phosphorylation

Introduction

Mig-6 (also called Ralt, Errfi1 and Gene 33) is a negative regulator of epidermal growth factor (EGF) signalling. Mig-6 binds to all EGF receptor (EGFR) family members and inhibits their tyrosine kinase activity (Anastasi *et al*, 2003). Mig-6 is induced by stimulation with fetal calf serum, insulin, and growth factors, including EGF, as an immediate early-response gene (Zhang and Vande Woude, 2007). Transcription of *Mig-6* is also induced by various stresses (Makkinje *et al*, 2000). Mig-6 functions as a feedback inhibitor of EGFR family signalling via its induction by the Ras/mitogen-activated protein kinase (MAPK) pathway (Fiorentino *et al*, 2000; Hackel *et al*, 2001; Anastasi *et al*, 2003; Xu *et al*, 2005; Anastasi *et al*, 2007).

Overexpression of Mig-6 leads to inhibition of EGFR autophosphorylation, and reduces MAPK activity (Anastasi *et al*, 2003; Xu *et al*, 2005; Anastasi *et al*, 2007). Mig-6 binds to EGFR family tyrosine kinases via its EGFR-binding domain (BD) and acts as a specific inhibitor of their signalling, while Mig-6 is suggested to contribute several biochemical functions as a multi-adaptor protein with many interactive domains. It is reported that Mig-6 binds to the GTP-bound form of Cdc42 via the CRIB domain and activates stress-activated protein kinases (Makkinje *et al*, 2000). The binding of Mig-6 to Cdc42 inhibits the activity of Cdc42, resulting in the inhibition of hepatocyte growth factor-induced cell migration (Pante *et al*, 2005). It is also reported that the processed CRIB domain of Mig-6, which is derived by limited proteolytic processing, binds to IκB and competes with NFκB, resulting in the activation of NFκB and its signalling (Tsunoda *et al*, 2002; Mabuchi *et al*, 2005).

Downregulated expression of the *Mig-6* gene is observed in breast carcinomas, in which it correlates with reduced overall survival (Amatschek *et al*, 2004; Anastasi *et al*, 2005). *Mig-6* is also downregulated in other human cancers such as hepatocellular carcinomas (Reschke *et al*, 2010) and thyroid cancers. *Mig-6* expression correlates with survival and is an independent predictor of recurrence in papillary thyroid cancers (Ruan *et al*, 2008). Recently, it has been reported that the *Mig-6* gene is mutated in the human non-small-cell lung cancer cell lines NCI-H226 and NCI-H 322M, as well as in primary human lung cancer (Zhang *et al*, 2007). *Mig-6*-deficient mice show hyperactivation of endogenous EGFR and sustained signalling through the MAPK pathway, resulting in overproliferation and impaired differentiation of epidermal keratinocytes. Furthermore, *Mig-6*-deficient mice develop spontaneous tumours in various organs and are highly susceptible to chemically induced skin tumours. Inhibition of endogenous EGF signalling by the EGFR inhibitor gefitinib (Iressa), or replacement of wild type (WT) EGFR with a kinase-deficient EGFR, rescues the skin defects in *Mig-6*-deficient mice (Ferby *et al*, 2006). Therefore, Mig-6 plays a tumour suppressor role as a specific negative regulator of EGF signalling.

Although Mig-6 is known to be an important tumour suppressor through negative regulation of EGF signalling, its posttranslational modifications such as phosphorylation have not been fully elucidated (Fiorentino *et al*, 2000; Fiorini *et al*, 2002). It has been reported that EGF promotes tyrosine

*Corresponding author. Department of Biochemistry 1, Hamamatsu University School of Medicine, 1-20-1 Handayama, Higashi-ku, Hamamatsu 431-3192, Japan. Tel.: +81 53 435 2322; Fax: +81 53 435 2322; E-mail: kitamasa@hama-med.ac.jp

Received: 8 June 2011; accepted: 15 March 2012; published online: 13 April 2012

phosphorylation of Mig-6 by EGFR tyrosine kinase (Tong *et al*, 2008), the biological implications of which are unknown. Another report indicated that Mig-6 can bind the phospho-serine binding adaptor protein 14-3-3 via its consensus motif for 14-3-3 binding, but the responsible kinase has not been identified (Makkinje *et al*, 2000).

One of the kinases that phosphorylates at the 14-3-3 consensus motif is Chk1. If DNA stability is perturbed, Chk1 is activated by ATM/ATR and phosphorylates a Ser residue in the 14-3-3 motifs of human Cdc25A, B, and C (Niida and Nakanishi, 2006). Chk1 is essential not only for checkpoint activation but also for cell viability in the absence of DNA perturbation. *Chk1*-knockout mice show embryonic lethality at an early stage of development. *Chk1*-conditional knockout embryonic stem cells and somatic cells also died, even in the absence of DNA damage (Liu *et al*, 2000; Niida *et al*, 2005). These phenotypes indicate that Chk1 has an important role during normal cell proliferation. However, the DNA damage-independent functions of Chk1 have not been fully elucidated.

In the present study, we investigated phosphorylation of Mig-6 and found that it is phosphorylated by Chk1 *in vitro* and *in vivo*. Moreover, we identified the sites for Chk1 phosphorylation and investigated the functional regulation of Mig-6 via Chk1-mediated phosphorylation in EGF signalling.

Results

Effects of protein kinase inhibitors on Mig-6 phosphorylation

Mig-6 acts as a negative feedback regulator of EGF signalling. However, little is known about its posttranslational modifications or regulatory mechanisms. We first investigated phosphorylation of Mig-6 because many cellular proteins are regulated by phosphorylation. FLAG-Mig-6 was transfected into HEK293 cells and immunoprecipitated (IP) with anti-FLAG antibody, and then the cell lysate were IP and analysed by SDS–PAGE followed by a Phos-tag BTL phosphoprotein detection method (Figure 1A). The result indicated that Mig-6 is phosphorylated in these cells. To identify the responsible kinase, we tested various protein kinase inhibitors (Supplementary Table S1) in the *in vivo* phosphorylation assay. We found that phosphorylation of Mig-6 was decreased remarkably by the Chk1 inhibitor SB218078 (Figure 1B, Supplementary Figure S1). As shown in Figure 1B, 10 μM

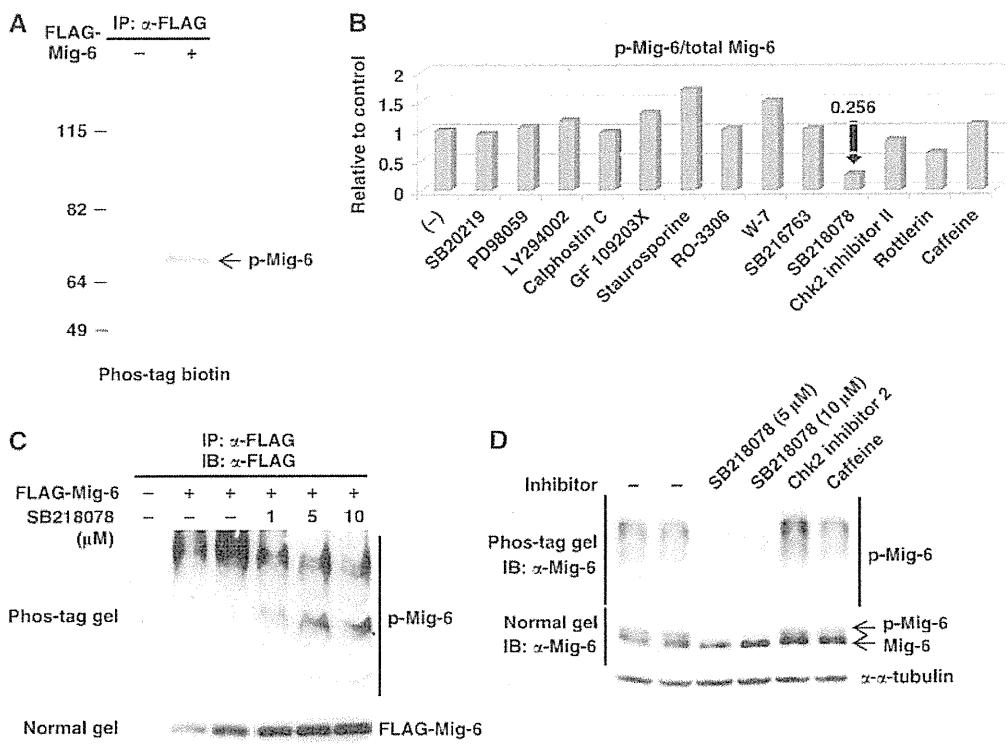

Figure 1 Effects of protein kinase inhibitors on Mig-6 phosphorylation *in vivo*. (**A**) Mig-6 is phosphorylated in HEK293 cells. pcDNA3-FLAG-Mig-6 was transfected into HEK293 cells. The whole cell lysates were IP with anti-FLAG M2 antibody and resolved by SDS–PAGE. Phosphorylated Mig-6 (p-Mig-6) was detected by a Phos-tag BTL system as described in Materials and methods. (**B**) Phosphorylation of Mig-6 is inhibited by Chk1 inhibitor (SB218078) *in vivo*. HEK293 cells were transfected with FLAG-Mig-6 and treated with the indicated kinase inhibitors for 3 h before harvesting. FLAG-Mig-6 was IP with anti-FLAG antibody from the cell lysates and p-Mig-6 was detected by the Phos-tag BTL system. Details of the kinase inhibitors are indicated in Supplementary Table S1. The intensities of the p-Mig-6 bands and total Mig-6 bands are indicated relative to the control (without inhibitor). (**C**) Phosphorylation of Mig-6 is inhibited by a Chk1 inhibitor in a dose-dependent manner. HEK293 cells were transfected with FLAG-Mig-6 and treated with the Chk1 inhibitor SB218078 at the indicated concentrations for 3 h before harvest. FLAG-Mig-6 was IP with anti-FLAG antibody from the cell lysate and separated by 6% Phos-tag SDS–PAGE (upper panel) or normal SDS–PAGE (lower panel) followed by IB with anti-FLAG antibody. (**D**) Phosphorylation of endo Mig-6 is inhibited by Chk1 inhibitor. MDA-MB-231 cells were treated without or with 5 or 10 μM SB218078, 10 μM Chk2 inhibitor 2, or 5 mM caffeine for 3 h. The cell lysates were separated by 6% Phos-tag SDS–PAGE (upper panel) or normal SDS–PAGE (lower panel) followed by IB with anti-Mig-6 antibody. Figure source data can be found with the Supplementary data.

SB218078 inhibited phosphorylation of Mig-6 to 25.6% of the control level. To confirm this, we performed Phos-tag SDS–PAGE analysis of Mig-6. Phosphorylation-dependent mobility shifts of Mig-6 were suppressed by SB218078 in a dose-dependent manner (Figure 1C). We next investigated whether the phosphorylation of endogenous Mig-6 (endo Mig-6) was also inhibited by the Chk1 inhibitor. Using MDA-MB-231 cells, in which Mig-6 is endogenously highly expressed, we confirmed that phosphorylation of endo Mig-6 was inhibited by Chk1 inhibitor, whereas Chk2 inhibitor 2 or caffeine (ATM/ATR inhibitor) did not affect it (Figure 1D). This suggests that Chk1 phosphorylates Mig-6 *in vivo*.

Chk1 phosphorylates Mig-6 in vitro

To examine whether Chk1 directly phosphorylates Mig-6, we performed an *in vitro* kinase assay. Recombinant (rec) Mig-6 protein was incubated with ^{32}P-labelled ATP and rec GST-Chk1 kinase at 30 °C for 30 min. As shown in Figure 2A, phosphorylation of Mig-6 was observed in the presence of Chk1 kinase, and autophosphorylation of Chk1 was also observed in the lane with Chk1. Moreover, both the Chk1-mediated phosphorylation of Mig-6 and autophosphorylation of Chk1 were inhibited by SB218078 in a dose-dependent manner (Figure 2B).

EGF stimulates Chk1-mediated phosphorylation of Mig-6

Previous studies have shown that Mig-6 functions as a feedback inhibitor of EGF signalling. Therefore, we next investigated whether Chk1-mediated phosphorylation of Mig-6 was associated with the EGF signalling pathway. As shown in Figure 2C, we found that phosphorylation of endo Mig-6 was

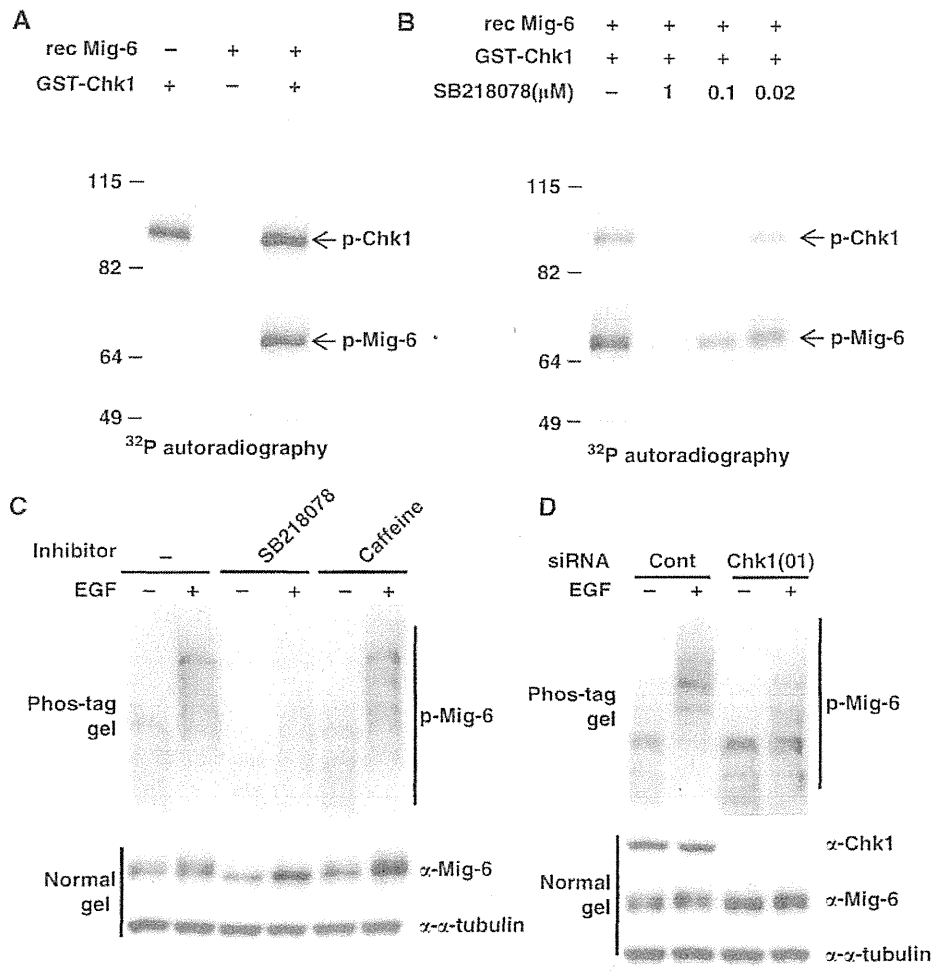

Figure 2 Chk1 phosphorylates Mig-6 after EGF stimulation. (**A**) *In vitro* phosphorylation of Mig-6. rec Mig-6 protein (0.1 μg) was incubated in 20 μl of kinase reaction buffer with ^{32}P-labelled ATP and 0.1 μg of purified rec GST-Chk1 kinase at 30°C for 30 min. The reaction was stopped by the addition of SDS sample buffer, then the proteins were separated by SDS–PAGE. p-Mig-6 was analysed by autoradiography. (**B**) Phosphorylation of Mig-6 is inhibited by a Chk1 inhibitor in a dose-dependent manner. rec Mig-6 proteins were pre-treated with SB218078 at the indicated concentration for 5 min at room temperature and then subjected to an *in vitro* kinase assay as described above. (**C**) EGF stimulation promotes phosphorylation of endo Mig-6. MDA-MB-231 cells were subjected to serum starvation for 16 h. Cells were pretreated with or without 10 μM SB218078 or 5 mM caffeine for 3 h, followed by stimulation with 20 ng/ml EGF for 15 min. Cells were harvested and the cell lysates were separated by 6% Phos-tag SDS–PAGE or normal SDS–PAGE, and subjected to IB with anti-Mig-6 antibody. (**D**) EGF-promoted phosphorylation of Mig-6 is suppressed by Chk1 depletion. MDA-MB-231 cells were transfected with an siRNA for human *Chk1* or a control siRNA (Cont) and serum starved for 16 h, then stimulated with 20 ng/ml EGF for 15 min. Cell lysates were separated by 6% Phos-tag SDS–PAGE or normal SDS–PAGE and analysed by IB with the indicated antibodies. Figure source data can be found with the Supplementary data.

promoted by EGF stimulation in MDA-MB-231 cells, and it was suppressed by the Chk1 inhibitor (Figure 2C, lane 2 versus lane 4), suggesting that Chk1 is involved in EGF-stimulated Mig-6 phosphorylation. Interestingly, caffeine, an ATM/ATR inhibitor, did not affect the phosphorylation of Mig-6 (Figure 2C, lane 2 versus lane 6) even though the same concentration of caffeine could counteract the phosphorylation of Chk1 induced by UV stimulation (Sarkaria *et al*, 1999; Mailand *et al*, 2000). Because caffeine did not affect EGF-stimulated Mig-6 phosphorylation, which was observed without genotoxic stress, it is likely that the Mig-6 phosphorylation by Chk1 is induced in a DNA damage-independent manner.

Next, we investigated the effect of Chk1 depletion on Mig-6 phosphorylation. Basal phosphorylation of Mig-6 in the absence of EGF stimulation was suppressed by depletion of Chk1 (Figure 2D, lane 1 versus lane 3). Moreover, EGF-stimulated Mig-6 phosphorylation was severely inhibited by depletion of Chk1 (Figure 2D, lane 2 versus lane 4). Furthermore, we performed a phosphatase-treatment experiment to prove that the smeared Mig-6 band on the Phos-tag gel was because of phosphorylation (Supplementary Figure S2B). We also demonstrated that the smeared Mig-6 band prepared from EGF-stimulated MDA-MB-231 cells on a Phos-tag gel did not indicate ubiquitylation (Supplementary Figure S2C). To confirm the Chk1-mediated Mig-6 phosphorylation, we designed and used another small interfering RNA (siRNA) oligo, *Chk1*(04). As shown in Figure 2D and Supplementary Figure S2A, depletion of Chk1 by both siRNA(01) and (04) attenuated phosphorylation of Mig-6. These results indicate that EGF stimulation promotes Chk1-mediated Mig-6 phosphorylation.

Analysis of the phosphorylation sites in Mig-6

Next, we tried to identify the Chk1-mediated phosphorylation site(s) in Mig-6. Chk1 often phosphorylates serine or threonine residues at an RxxS/T motif (O'Neill *et al*, 2002). After comparing the amino-acid sequences of Mig-6 between human, mouse, and rat, we selected five conserved serine residues as candidates. S249 and S251 are in the 14-3-3-BD, while S302, S334, and S369 are located in the AH domain, which is involved in binding to EGFR (Figure 3A). We substituted these serine residues with alanine to determine the Chk1 phosphorylation sites using an *in vitro* kinase assay with rec proteins. We found decreased phosphorylation in the S249/251A and S249/251/302/334/369A mutants but not in the S302/334/369A mutant using ^{32}P autoradiography as well as immunoblotting (IB) with anti-phospho-serine (Figure 3B, Supplementary Figure S3A). Moreover, the Chk1-mediated phosphorylation of S251A but not S249A mutant Mig-6 was apparently decreased compared with that of WT Mig-6 (Figure 3C). To confirm that S251 is a phosphorylation site *in vivo*, WT or S251A Mig-6 was transfected into HEK293 cells, which were then stimulated with EGF. As shown in Figure 3D, the phosphorylation-dependent mobility shift of the S251A mutant was smaller than that of WT Mig-6, suggesting that S251 is phosphorylated *in vivo*. At the same time, we found that at least one of S302/334/369 was phosphorylated following EGF stimulation (Supplementary Figure S3B). We tried to generate a Mig-6 phospho-S251-specific antibody to enable further confirmation, but unfortunately were unsuccessful.

We next demonstrated the phosphorylation sites of Mig-6 using mass spectrometry (MS). HEK293 cells were transfected with FLAG-Mig-6 and stimulated with EGF. Mig-6 protein was prepared by immunoprecipitation with anti-FLAG antibody from the lysates, separated by SDS–PAGE and analysed by liquid chromatography (LC)-MS. We identified S251-phosphorylated peptides such as SHpSGPAGSFNKPAIR, indicating that Mig-6 was phosphorylated at S251 *in vivo* (Supplementary Figure S4A). Next, endo Mig-6 prepared from MDA-MB-231 cells treated with EGF was subjected to LC-MS analysis. We identified S251-phosphorylated peptides such as SHpSGPAGSFNKPAIR, indicating that endo Mig-6 was also phosphorylated at S251 (Figure 3E). The numbers of identified phosphorylated peptides in the exogenous FLAG-Mig-6 (exo Mig-6) and the endo Mig-6 protein (endo Mig-6) are indicated in Figure 3F. Because phospho-S251-containing peptides were commonly detected in both exo Mig-6 and endo Mig-6, we believe that S251 is an *in vivo* phosphorylation site in Mig-6.

As shown in Figure 3F, not only S251, but also S273, S276, S302, and S326 were phosphorylated in both exo and endo Mig-6. These sites might include not only Chk1-mediated phosphorylation sites but also Chk1-independent phosphorylation sites. S251 and S302 are located within a putative consensus motif for Chk1 (R-X-X-S/T), whereas S273, S276, and S326 are not. To determine the Chk1-mediated phosphorylation sites, rec Mig-6 protein was phosphorylated by GST-Chk1 *in vitro* followed by LC-MS analysis. We found that S251 and S302, but not S273, S276, or S326, were phosphorylated by Chk1 *in vitro* (Figure 3F, Supplementary Figure S4B). Taken together, Chk1 could directly phosphorylate both S251 and S302 in Mig-6, suggesting that they are major Chk1-mediated phosphorylation sites in Mig-6.

Effects of Chk1-mediated phosphorylation of Mig-6 S251 on EGF signalling

To determine the physiological relevance of Mig-6 phosphorylation, we investigated the effect of substitution at the Chk1-mediated phosphorylation sites on Mig-6 function as a negative feedback inhibitor of EGF signalling. WT, S251A, and S251E (phospho-mimic form) Mig-6 were transfected into HEK293 cells, and the cells were treated with or without EGF. Phosphorylation of EGFR was analysed by IB with anti-phospho-EGFR or anti-phospho-tyrosine antibody. Similar to NIH-EGFR (Anastasi *et al*, 2007) and Cos-7 cells (Zhang *et al*, 2007), we confirmed that WT Mig-6 suppressed autophosphorylation of EGFR in EGF-stimulated HEK293 cells (Supplementary Figure S5A, lane 2 versus lane 4). The S251A mutant suppressed this autophosphorylation much more strongly than did WT Mig-6 (Supplementary Figure S5A, lane 4 versus lane 6). In contrast, autophosphorylation of EGFR was partially restored in cells expressing the S251E mutant (Supplementary Figure S5A, lane 6 versus lane 8, and B), suggesting that phosphorylation of S251 in Mig-6 negatively regulates the inhibitory activity of Mig-6 on EGF signalling.

To investigate the effect of Mig-6 S251 phosphorylation on cell growth, we performed proliferation assays. Expression of the S251A mutant markedly inhibited the proliferation of HEK293 cells, whereas the WT and S251E mutant did not affect cell growth (Supplementary Figure S5C). This is presumably because WT Mig-6 is phosphorylated at S251 in HEK293 cells in normal culture medium without further stimulation by EGF.

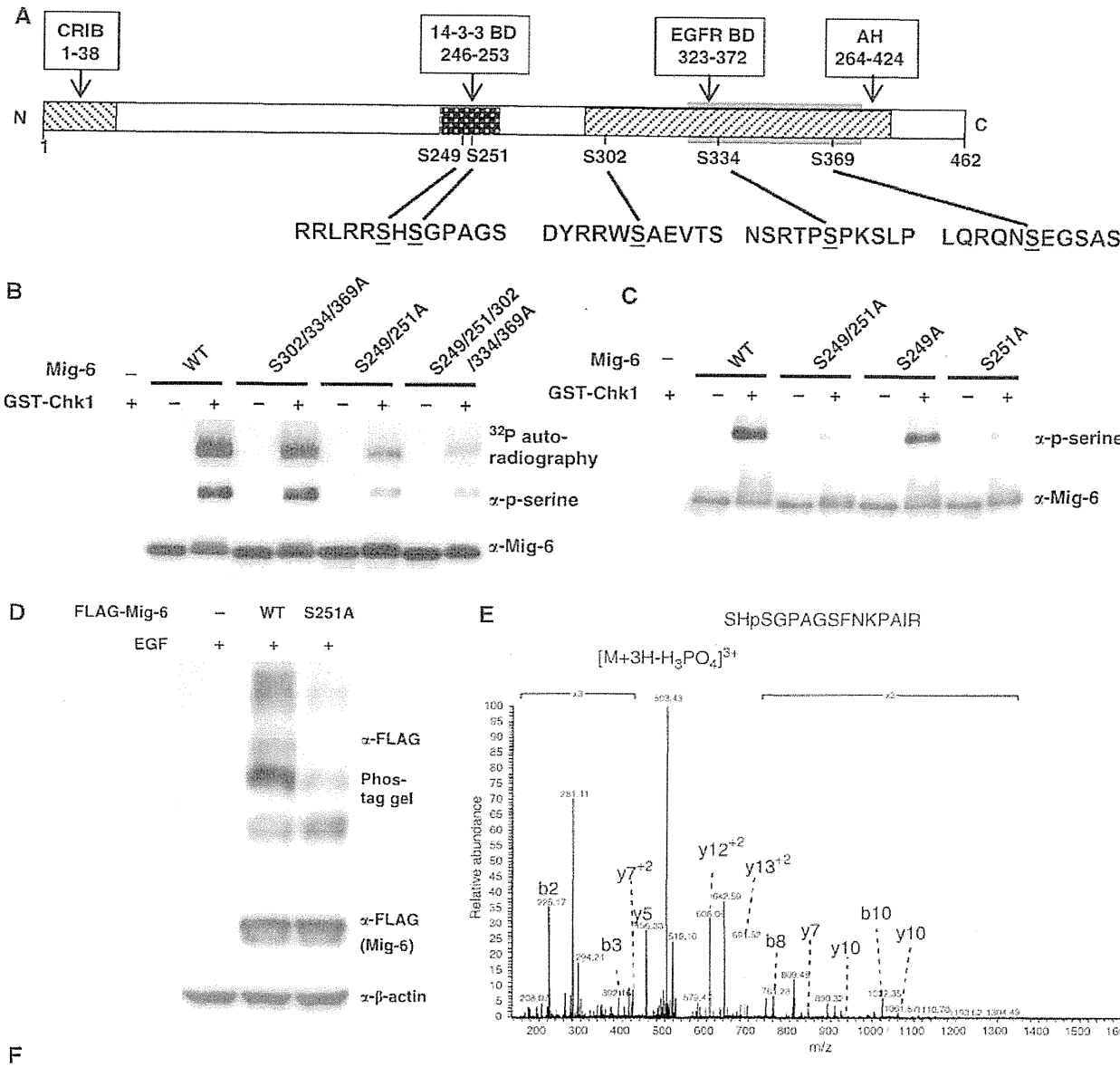

F

	Phosphorylated amino acid residues (number of identified peptides)																			
	T17	S91	T127	S136	S138	S249	S251	S265	S273	S276	S302	S307	S311	S326	S328	S369	Y394	T436	S457	S461
exo Mig-6		1	4	2		2	27	4	16	17	8	1	9	16	1	7		1		9
endo Mig-6							6		3	1	9			3			1			
rec Mig-6	1				3		9				3					2			4	

Figure 3 Analysis of the phosphorylation sites in Mig-6. (**A**) Primary structure of Mig-6 and schematic representation of its point mutation sites. (**B, C**). *In vitro* Chk1 phosphorylation site(s) analysis of Mig-6. WT or mutant rec Mig-6 proteins (0.1 μg) were incubated in 20 μl of kinase buffer with ^{32}P-labelled ATP and 0.1 μg of purified rec GST-Chk1 kinase at 30 °C for 30 min. p-Mig-6 was analysed by autoradiography or IB with anti-phospho-serine antibody. (**D**) Comparison of phosphorylation status between WT and S251A mutant Mig-6 in HEK293 cells. WT or S251A mutant FLAG-Mig-6 was transfected into HEK293 cells. After 16 h serum starvation, cells were stimulated with 20 ng/ml EGF for 15 min and then harvested. Whole cell lysates were separated by 6% Phos-tag SDS–PAGE (upper panel) or normal SDS–PAGE and analysed by IB with the indicated antibodies. (**E**) Identification of S251 phosphorylation of endo Mig-6 using MS. Quiescence was induced in MDA-MB-231 cells by 16-h serum starvation; the cells were then treated with 20 ng/ml EGF for 15 min and harvested. Endo Mig-6 was IP with anti-Mig-6 antibody from the lysate and separated by SDS–PAGE. After tryptic digestion of the Mig-6 band, phosphorylated peptides were analysed by LC-MS. The spectrum of the charged ions (m/z 503.38) shows that S251 is phosphorylated in the indicated peptide (top right). b ions, fragmentation ions containing the amino terminus of the peptide; y ions, fragmentation ions containing the carboxy terminus of the peptide. (**F**) Phosphorylation sites in Mig-6. The number of identified phosphorylated peptides in endo Mig-6 are indicated. exo Mig-6 protein IP from EGF-stimulated HEK293 cells transfected with FLAG-Mig-6 was also analysed by MS. rec Mig-6 protein phosphorylated *in vitro* by GST-Chk1 (rec Mig-6) was separated by SDS–PAGE and analysed by MS. Figure source data can be found with the Supplementary data.

For further information, we performed rescue experiments using siRNA-resistant Mig-6 wild type, S251A, or S251E. MDA-MB-231 cells were infected with retrovirally encoded Mig-6 wild type, S251A, or S251E, and then treated with an siRNA-targeting *Mig-6*. After EGF stimulation, autophosphorylation of EGFR was analysed by IB. As shown in Figure 4A and B and Supplement Figure S5D, treatment with a *Mig-6* siRNA increased the autophosphorylation of EGFR to ~120% of control levels. Introduction of WT Mig-6 inhibited the autophosphorylation of EGFR to 66% of that for the empty vector control. The S251A mutant suppressed the autophosphorylation of EGFR significantly more strongly than did WT Mig-6. Because Mig-6 is highly phosphorylated in EGF-stimulated MDA-MB-231 cells, the effect of S251E on autophosphorylation was almost the same as that of WT Mig-6. Next, we performed rescue experiments on cell proliferation using siRNA-resistant Mig-6 wild type, S251A, or S251E. As described above, MDA-MB-231 cells were infected with retrovirally encoded Mig-6 wild type, S251A, or S251E, and then treated with siRNA for *Mig-6*. Then, cell proliferation assays were performed. As shown in Figure 4C, the doubling time of cells expressing S251A was significantly prolonged compared with that of the WT and the S251E mutant. Because Mig-6 is highly phosphorylated in MDA-MB-231 cells in normal culture conditions, it is consistent that the effect of S251E on cell proliferation was almost the same as that of WT Mig-6. Moreover, we obtained almost the same data using HEK293 cells that were transfected with Mig-6 plasmids (Supplementary Figure S5). These results were reproducible in three independent experiments, and the effect of the S251A mutant was always moderate. Therefore, we conclude that phosphorylation of Mig-6 S251 is involved in the regulation of EGF signalling.

We tested additional phosphorylation site such as S302 in which phosphorylation as well as S251 was identified by MS in *in vitro*, *in vivo*, and endogenous status (Figure 3F). As shown in the Supplementary Figure S6A, S302/334/369A mutant showed the same inhibitory effect on autophosphorylation of EGFR as WT Mig-6 in HEK293 cells. Furthermore, retroviral expression of Mig-6 S302A had no effect on both autophosphorylation of EGFR and proliferation in MDA-MB-231 cells (Supplementary Figure S6, B–D). Taken together, these results suggest that phosphorylation of Mig-6 S251 but not S302 is important for its inhibitory function on EGF signalling and regulation of cell proliferation.

EGF stimulation promotes phosphorylation of Chk1 at S280

To clarify the Chk1 modification in EGF signalling pathway, we performed quantitative phospho-proteome analysis of EGF-stimulated HeLa cells using LC-MS, a technique termed phospho-iTRAQ (Leitner and Lindner, 2009). Phosphorylation of EGFR (Y1172, Y1192) and PRAS40 (T246) indicating Akt activity peaked at 5 min after stimulation and then oscillated.

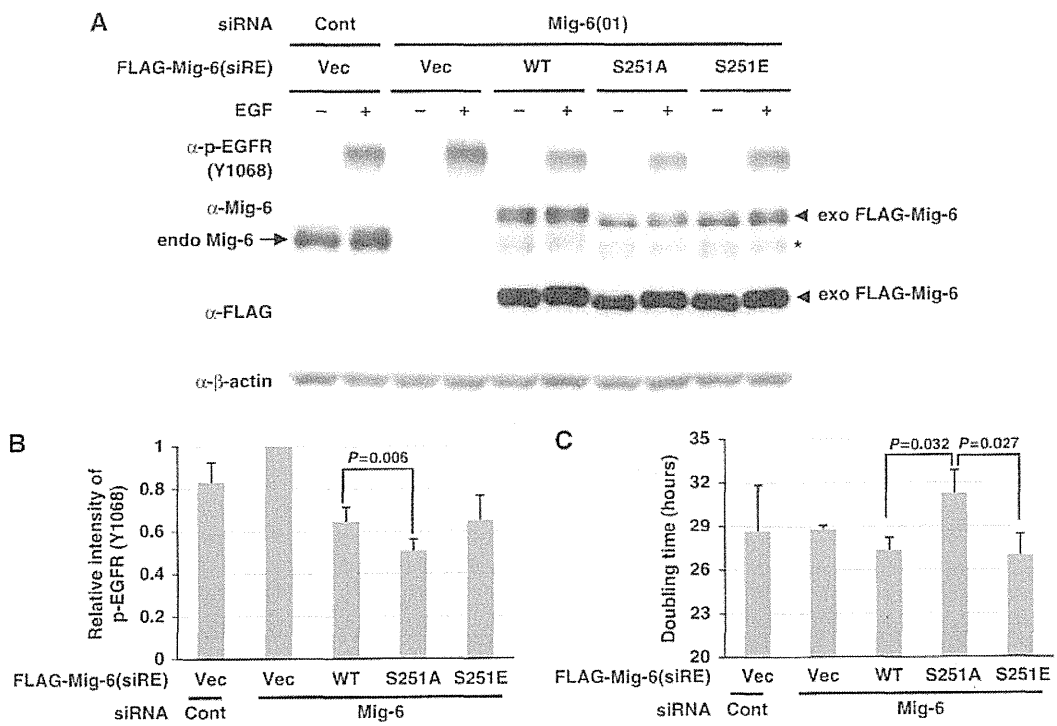

Figure 4 Effect of Mig-6 S251 phosphorylation on EGF signalling. (**A**) Effect of Mig-6 S251 mutation on EGF signalling. MDA-MB-231 cells were infected with retroviruses encoding Mig-6 wild type, S251A, or S251E, and then treated with an siRNA-targeting *Mig-6* or a control siRNA (Cont). After 16 h serum starvation, cells were stimulated with 20 ng/ml EGF, then harvested 15 min later. Cell lysates were separated using SDS–PAGE followed by IB. The asterisk indicates retrovirally expressed Mig-6 protein without the FLAG-tag, which is translated using the original first methionine of the *Mig-6* cDNA. (**B**) The intensity of p-EGFR (Y1068) protein in each condition in (**A**) was quantified by image analysis. The data from triplicate experiments were evaluated statistically and are shown graphically relative to the data from the vector only. (**C**) Effect of S251 status on cell growth. MDA-MB-231 cells were infected with retrovirally encoded Mig-6 wild type, S251A, or S251E, and then treated with an siRNA for *Mig-6* or a control siRNA (Cont). Cell proliferation assays were performed. The doubling times were calculated and are shown graphically. Figure source data can be found with the Supplementary data.

Chk1 became phosphorylated at S280 from 10 min after stimulation (Supplementary Figure S7, A–C). This suggests that phosphorylation of S280 in Chk1 might be induced via the PI3K/Akt pathway, which is consistent with a previous report that PI3K activation promotes phosphorylation of Chk1 at S280 (Puc *et al*, 2005). These authors concluded that S280-phosphorylated Chk1 is preferentially tethered in the cytoplasm. We then investigated whether EGF signalling promoted S280 phosphorylation of Chk1 in MDA-MB-231 cells. We found that EGF promoted phosphorylation of Chk1 S280, with a similar duration to Mig-6 phosphorylation, whereas Chk1 S345 was not upregulated (Figure 5A). As shown in Figure 5B, depletion of neither ATM nor ATR affected EGF-dependent S280 phosphorylation of Chk1. This is consistent with the data shown in Figure 2C, in which the ATM/ATR inhibitor caffeine did not affect the phosphorylation of Mig-6.

Next, we investigated the PI3-kinase pathway (Figure 5C–E). The PI3K inhibitor LY294002 inhibited the phosphorylation of not only Akt S473 but also Chk1 S280 and Mig-6 (Figure 5C). Similarly, Akt inhibitor IV inhibited S280 phosphorylation of Chk1 in a dose-dependent manner (Figure 5D). Depletion of p70S6K, a downstream kinase of Akt, inhibited EGF-induced S280 phosphorylation of Chk1 (Figure 5E). To address whether Akt or p70S6K phosphorylates Chk1 at S280 directly, we performed *in vitro* phosphorylation experiments using recombinant proteins. As shown in Figure 5F, it is p70S6K, but not Akt, phosphorylated Chk1 directly. These results suggest that p70S6K, a downstream kinase of Akt, is involved in phosphorylation of Chk1 at S280 via the EGFR-PI3K/Akt pathway.

Chk1 phosphorylates and inhibits Mig-6, acting as a positive regulator of EGF signalling

We next investigated the physiological relevance of EGF-promoted phosphorylation of Mig-6 by Chk1. We transfected MDA-MB-231 cells with an siRNA for *Chk1*(01) or *Mig-6*(01), or a control siRNA, and then stimulated with EGF. EGF promoted phosphorylation of EGFR, Chk1 S280, and ERK from 5 min after stimulation, peaked at 15–30 min, and reduced from 1 h. Depletion of Chk1 attenuated EGFR phosphorylation and ERK phosphorylation at 5–30 min after EGF treatment. In contrast, depletion of Mig-6 enhanced EGFR phosphorylation and ERK phosphorylation in the same period (Figure 6, Supplementary Figure S9). These tendencies were reproducible in three independent experiments (Figure 6 and Supplementary Figure S8). Moreover, another *Chk1* siRNA oligo (04) showed the same result as did *Chk1* siRNA oligo (01) (Supplementary Figure S10). These data indicate that depletion of Chk1 results in a decreased phosphorylation of EGFR. Therefore, Chk1 may play a role as a positive regulator of EGF signalling via phosphorylation of Mig-6.

Next, we investigated whether phosphorylation of Mig-6 affects activation of other EGFR family members. As shown in Figure 7A, depletion of Mig-6 facilitated the phosphorylation of not only EGFR but also of ERBB2 and ERBB3 (Figure 7A, lanes 2 versus 6). Moreover, we found that depletion of Chk1 inhibited the phosphorylation of not only EGFR but also of ERBB2 and ERBB3 (Figure 7A, lanes 2 versus 4). These results suggest that Chk1 is also involved in the activation of other EGFR members via phosphorylation of Mig-6.

To demonstrate that Mig-6 is a downstream target of Chk1 in EGF signalling, we investigated the effect of Mig-6 depletion on the activation of EGFR promoted by Chk1 depletion. The EGF-dependent activation of EGFR was inhibited by Chk1 depletion, but rescued by co-depletion of Mig-6 (Figure 7B). Next, we investigated the relationship between Mig-6 and Chk1 on cell proliferation and found that cell growth was also suppressed by Chk1 depletion, but was rescued by co-depletion of Mig-6 (Figure 7C and D). Our results suggest that Chk1 phosphorylates Mig-6 on S251, resulting in the inhibition of Mig-6, and is involved in the regulation in EGF signalling as a positive regulator (Figure 7E).

Discussion

Mig-6 as a novel target of Chk1

ATM-Chk2 and ATR-Chk1 play critical roles in the DNA damage stress response pathway (Zhou and Elledge, 2000). In particular, the ATR-Chk1 axis is essential to block the cell cycle through inhibition of the Cdc25 family. Chk1 also regulates Cdc25A (Chen *et al*, 2003; Lam and Rosen, 2004; Uto *et al*, 2004) and Cdc25B activities throughout an unperturbed cell cycle (Schmitt *et al*, 2006). In contrast to the well-characterized role of Chk1 in the checkpoint pathway, little is known about how Chk1 acts in normal cell cycle progression. The kinase activity of Chk1 is maintained during the cell cycle. Recently, Shimada *et al* (2008) reported that Chk1 bound chromatin and induced cdk1 and cyclin B transcripts by histone H3 Thr11 phosphorylation in the absence of DNA damage. Here, we revealed a novel function of Chk1. We found that the EGFR inhibitor Mig-6 is a novel target of Chk1 under normal cell cycle conditions and in the absence of DNA damage. We noticed that both exo Mig-6 and endo Mig-6 were phosphorylated in living cells. Mig-6 has a PLTP consensus sequence for phosphorylation by ERKs (Gonzalez *et al*, 1991), a PPLTPI consensus sequence for phosphorylation by cyclin D1-Cdk4 (Kitagawa *et al*, 1996), PKC (S/T-XR/K) (Woodgett *et al*, 1986), and several potential sites for phosphorylation by Chk1 (O'Neill *et al*, 2002). We found that Chk1 is a candidate Mig-6 kinase using various kinase inhibitors and demonstrated this function by depletion of Chk1. We also found that EGF stimulation promoted phosphorylation of Mig-6 in the absence of DNA damage, and that Mig-6 phosphorylation was severely suppressed by a Chk1 inhibitor or by silencing Chk1 by treatment with siRNA. Depletion of ATM or ATR as well as treatment with ATM/ATR inhibitor caffeine did not affect EGF-stimulated Mig-6 phosphorylation. Our results indicated that Chk1 could phosphorylate Mig-6 by EGF stimulation, not via ATR, in a DNA damage-independent manner. It has been reported that S345 and S317 are the main phosphorylation sites of Chk1 in the DNA damage response. We confirmed that phosphorylation of S345 and S317 was upregulated upon DNA damage induced by UV light in MDA-MB-231 cells, but not by EGF stimulation (Figure 5C and unpublished observations). In contrast, phosphorylation of Chk1 at S280 was apparently promoted by EGF signalling. Puc *et al* (2005) indicated that PI3K activation promotes the phosphorylation of Chk1 at S280 and that S280-phosphorylated Chk1 is preferentially tethered in the cytoplasm. We believe that cytoplasmically

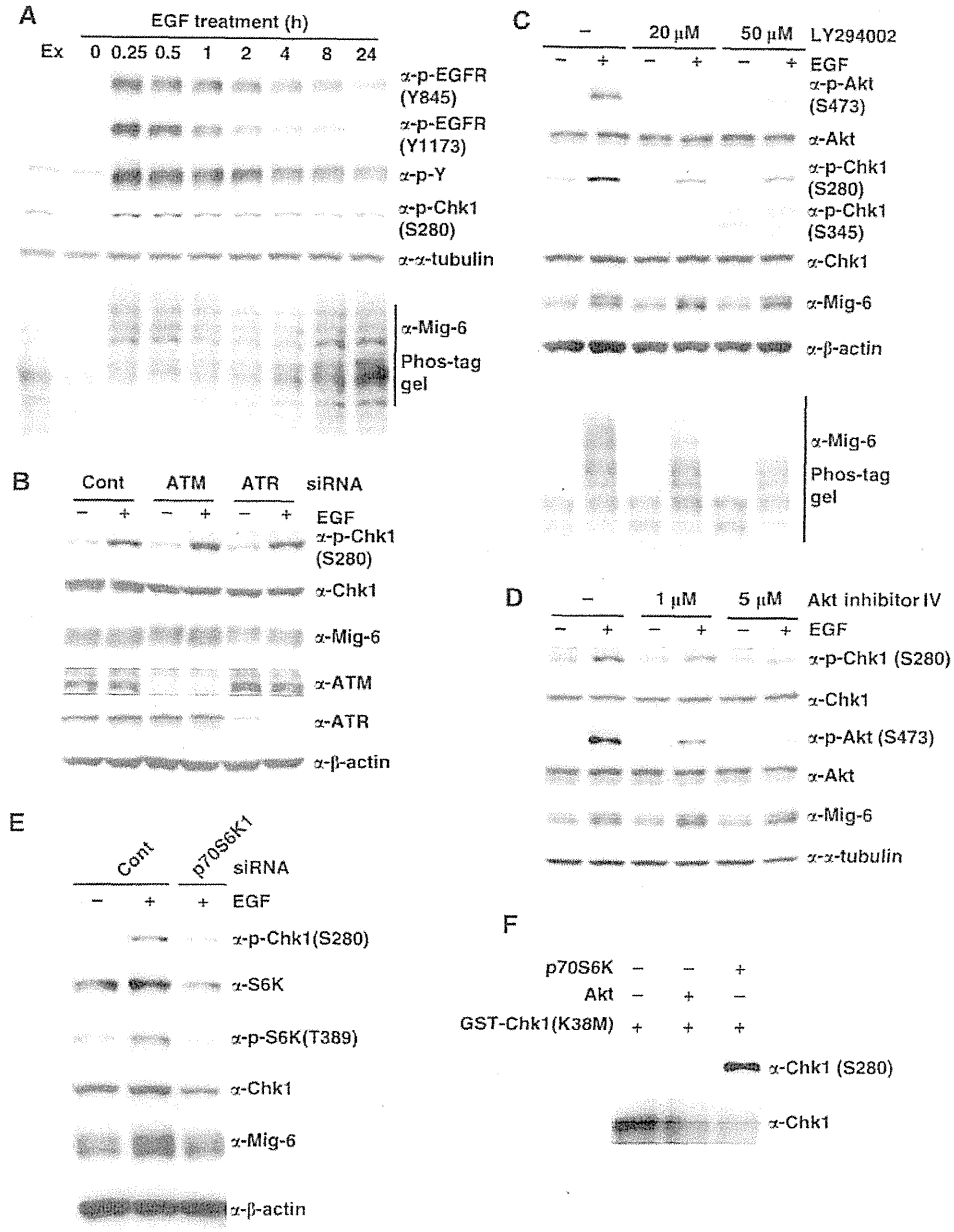

Figure 5 Phosphorylation of Chk1 at S280 is promoted by EGF stimulation via the PI3K pathway. (**A**) Time course of phosphorylated proteins in MDA-MB-231 cells treated with EGF. MDA-MB-231 cells were subjected to serum starvation for 16 h, then treated with 20 ng/ml EGF for the indicated times. The cell lysates were analysed by IB with the indicated antibodies (Ex, without serum starvation and EGF stimulation). (**B**) Depletion of ATM/ATR had no effect on S280 phosphorylation of Chk1. MDA-MB-231 cells were transfected with an siRNA for human *ATM* or *ATR* or a control siRNA (Cont). Quiescence was induced by 16-h serum starvation, and then the cells were stimulated with 20 ng/ml EGF for 15 min. The cell lysates were analysed by IB with the indicated antibodies. (**C**) Effect of a PI3K inhibitor on Chk1 phosphorylation. MDA-MB-231 cells were subjected to serum starvation for 16 h. Cells were pretreated with or without the PI3K inhibitor LY294002 for 1 h, followed by stimulation with 20 ng/ml EGF for 15 min. Cell lysates were separated by normal SDS–PAGE or 6% Phos-tag SDS–PAGE and immunoblotted. (**D**) Effect of an Akt inhibitor on Chk1 phosphorylation. MDA-MB-231 cells were made quiescent by 16-h serum starvation, pretreated with or without Akt inhibitor IV for 1 h, then stimulated with 20 ng/ml EGF for 15 min. The cell lysates were analysed by IB with the indicated antibodies. (**E**) Depletion of p70S6k1 inhibits Chk1 phosphorylation. MDA-MB-231 cells were transfected with an siRNA for human *S6K1* or a control siRNA (Cont), then made quiescent by 16-h serum starvation. Cells were harvested after EGF stimulation, and subjected to IB with the indicated antibodies. (**F**) *In vitro* phosphorylation of Chk1 S280 by Akt2 and p70S6K. rec GST-Chk1 (kinase-deficient mutant K38M) proteins were incubated in 20 μl of kinase reaction buffer with 50 μM ATP and 1 μl Akt2 (Abcam, ab79798) or p70S6K (Abcam, ab84798) at 30°C for 30 min. The reaction was stopped by the addition of SDS sample buffer, then the proteins were separated using SDS–PAGE followed by IB with indicated antibodies. Figure source data can be found with the Supplementary data.

localized Chk1 is susceptible to interaction with Mig-6. Moreover, EGFR activity suppressed by Chk1 depletion was rescued by Mig-6 depletion. Therefore, Mig-6 is a downstream target for phosphorylation by Chk1 in a DNA damage-independent manner. The contribution of the Chk1-Mig-6 pathway to EGFR activation is significant and reproducible but moderate, because EGF signalling is regulated by multiple mechanisms. We believe that the

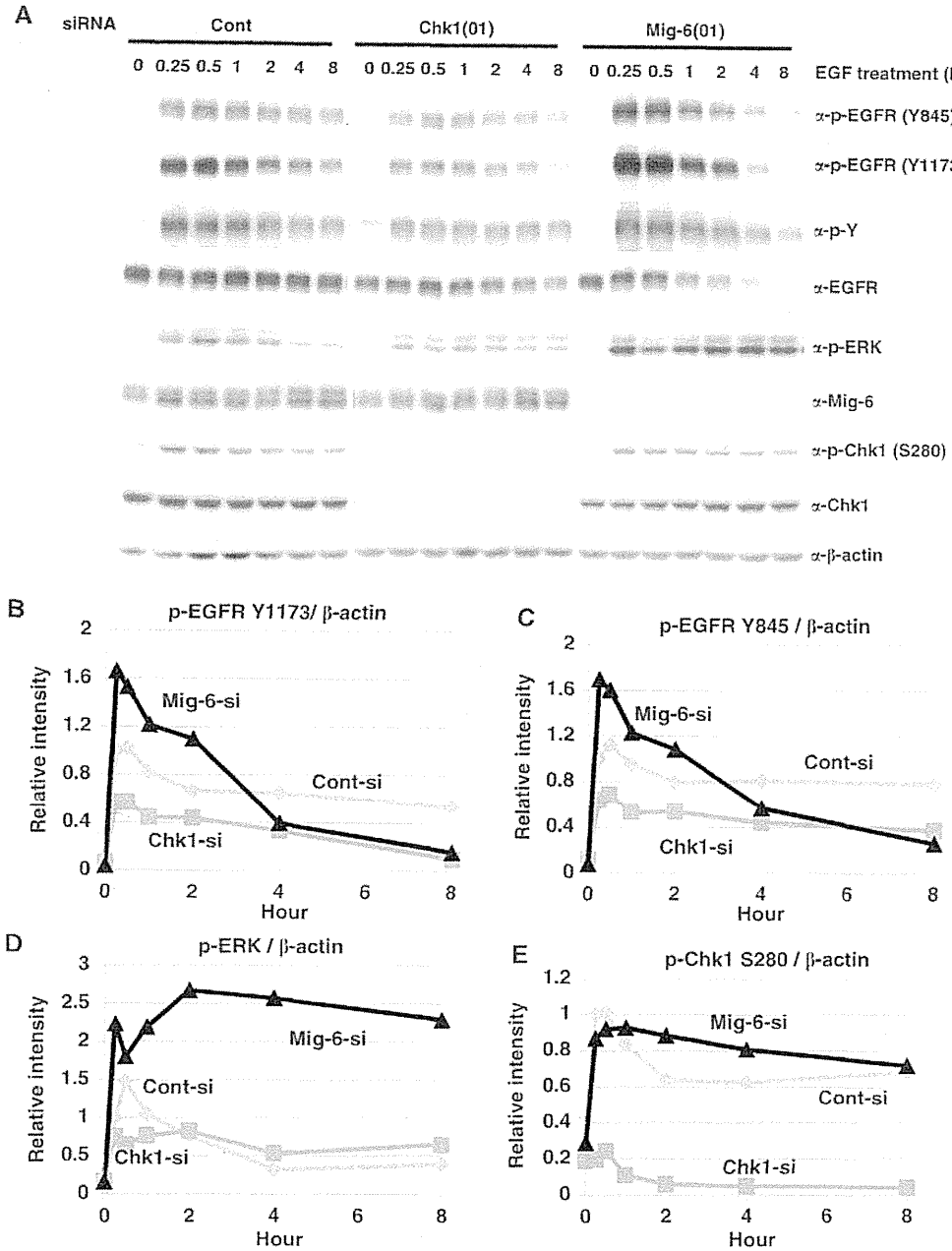

Figure 6 Effect of Chk1 depletion on EGF signalling. (**A**) EGF-promoted phosphorylation of EGFR is suppressed by Chk1 depletion. MDA-MB-231 cells were transfected with an siRNA for *Chk1* or *Mig-6*, or a control siRNA (Cont), serum starved for 16 h, then stimulated with 20 ng/ml EGF for the indicated times. Cell lysates were separated by SDS–PAGE and analysed by IB with the indicated antibodies. (**B–E**). The intensities of the indicated phosphorylated proteins were quantified by image analysis and are shown graphically. Three independent experiments were performed as shown in Supplementary Figure S8. Figure source data can be found with the Supplementary data.

Chk1-Mig-6 pathway modulates EGFR activation as one of the regulatory mechanisms of EGF signalling.

Chk1-mediated phosphorylation sites in Mig-6

Tyrosine phosphorylation of Y394 in Mig-6 has been reported by Guha *et al* (2008), which is consistent with our MS data for endo Mig-6. However, serine/threonine phosphorylation of Mig-6 has not been reported at all. Our results indicated that S251 and S302 are two major phosphorylation sites of Mig-6 by Chk1. However, substitution of serine 302 to alanine did not affect its inhibitory activity against EGFR comparing with WT Mig-6 (Supplementary Figure S6). Therefore, we presume that S251 is the main functional target site for phosphorylation by Chk1 in response to EGF stimulation.

S251 is located in the 14-3-3 binding site (R-S-X-S-X-P) (Muslin *et al*, 1996) in Mig-6; an interaction between exo Mig-6 and 14-3-3 was reported by Makkinje *et al* (2000). Our data indicated that WT Mig-6 bound to 14-3-3β, δ, and ξ (Supplementary Figure S11A), whereas S251A mutant showed a low binding affinity to 14-3-3β and ξ but not δ. Moreover,

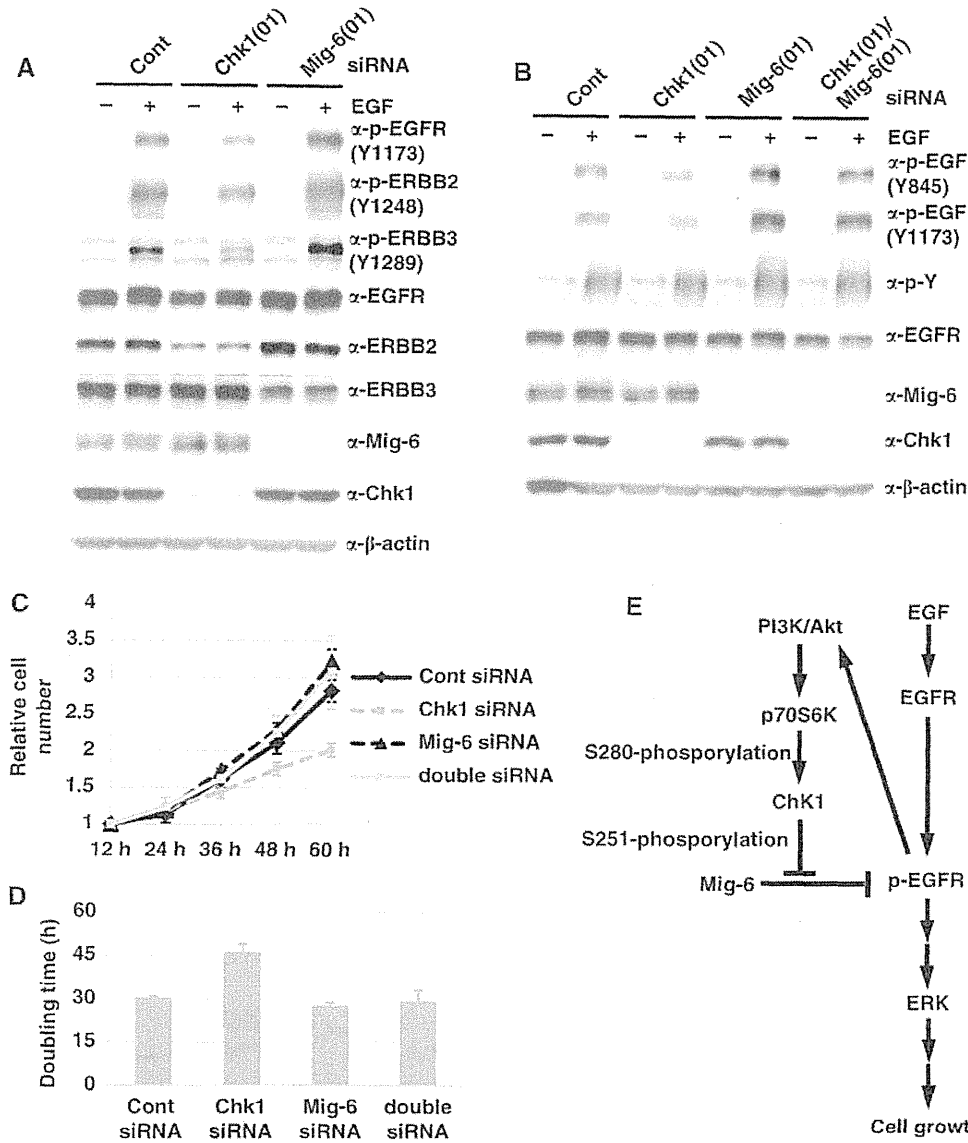

Figure 7 Mig-6 is a downstream target for Chk1 in EGF signalling. (**A**) Effect of Chk1 knockdown on activation of ERBBs. MDA-MB-231 cells were transfected with an siRNA for human *Chk1* or *Mig-6* or a control siRNA (Cont). Quiescence was induced by 16-h serum starvation, then the cells were stimulated with 20 ng/ml EGF for 15 min. The cell lysates were analysed by IB with the indicated antibodies. (**B**) Effect of Mig-6 depletion on activation of EGFR promoted by Chk1 depletion. MDA-MB-231 cells were transfected with siRNA for *Chk1* and/or *Mig-6* or a control siRNA (Cont), serum starved for 16 h, then stimulated with 20 ng/ml EGF for 15 min. Cell lysates were separated by SDS–PAGE and analysed by IB with the indicated antibodies. (**C**, **D**) Involvement of Chk1 in cell growth as an upstream regulator of Mig-6. MDA-MB-231 cells were transfected with siRNA for *Chk1* and/or *Mig-6* or a control siRNA (Cont). Cell numbers were measured at the indicated times (**C**). The doubling times were calculated from the growth curves (**D**). Error bars indicate the s.d. of three independent experiments. (**E**) A model of regulation of EGF signalling by Chk1-mediated phosphorylation of Mig-6. Figure source data can be found with the Supplementary data.

depletion of Chk1 attenuated the binding of Mig-6 to 14-3-3ξ, but not to 14-3-3β and δ (Supplementary Figure S11B). Therefore, phosphorylation of S251, which is located in the putative 14-3-3 binding sequence in Mig-6, may be involved in binding of Mig-6 to 14-3-3ξ.

We noticed that no effect of Mig-6 phosphorylation on its association with EGFR family members was detected using co-immunoprecipitation (data not shown). We speculate that Chk1-mediated phosphorylation of Mig-6 may increase activation of the EGFR family members via some conformational change in the EGFR-Mig-6 complex. Alteration in the binding of Mig-6 to 14-3-3ξ may affect the conformation of Mig-6-EGFR family complex, although further study is required to clarify the mechanism.

Regulation of EGF signalling by the Chk1-Mig-6 pathway

Because Mig-6 is downregulated in many tumour cells, these cells may escape from Mig-6-mediated growth control. EGF signalling is negatively regulated by Mig-6 in cells that express a normal level of Mig-6. Attenuation of Mig-6 activity may be required for efficient activation of EGFR, leading to the accelerated cell growth in these cells. EGF stimulation may promote Chk1-mediated phosphorylation of Mig-6 to

negate the EGFR repression. It has been reported that EGF activates the PI3K/Akt pathway (Klein and Levitzki, 2009), and that lack of the PI3K inhibitor PTEN promotes phosphorylation of Chk1 at S280, thereby sequestering S280-phosphorylated Chk1 in the cytoplasm (Puc *et al*, 2005; Jean *et al*, 2007). Our results also indicated that EGF stimulation induced phosphorylation of Chk1 at S280, which could be inhibited by a PI3K inhibitor or an Akt inhibitor. Moreover, we found that p70S6K, a downstream kinase of Akt, is involved in the phosphorylation of Chk1 at S280 via EGFR-PI3K/Akt pathway. Therefore, we speculate the following new insight into the regulation of EGF signalling, EGF stimulation activates the PI3K/Akt pathway to phosphorylate Chk1 at S280 in the early stages of EGF signalling. S280-phosphorylated Chk1 is sequestered in the cytoplasm and phosphorylates Mig-6 at S251. Then, the inhibitory activity of Mig-6 on EGFR activation is attenuated by the S251 phosphorylation, and thereby EGFR is fully activated to promote downstream signal transduction and cell growth (Figure 7E). Attenuation of Mig-6 activity may be required for efficient activation of EGFR in the early stage. In the late stages of EGF signalling, transcriptional induction of *Mig-6* is increased and Mig-6 is gradually dephosphorylated; EGFR phosphorylation and the downstream signal transduction is therefore attenuated, preventing from overactivity. (Figure 5A). In summary, Chk1 functions as a positive regulator in the early stages of EGF signalling.

Because the EGFR pathway is an important molecular target for cancer therapy, many EGFR tyrosine kinase inhibitors are being tested for an ability to prevent EGF-dependent cancer cell growth. We believe that regulation of the EGFR-Mig-6 pathway is also applicable to cancer therapy. Chk1 kinase inhibitors have been presented as sensitizers against cancer chemotherapy to avoid Chk1-mediated cell cycle arrest (Xiao *et al*, 2005). In the present study, we found that Chk1 promoted EGF signalling via Mig-6 inhibition. Depletion of Chk1 and Chk1 inhibition suppressed cancer cell growth. Therefore, Chk1 inhibitors may be useful to inhibit EGF-dependent cell growth in Mig-6-positive cancer cells.

Materials and methods

Cell culture

The human cell lines HEK293, HeLa, MDA-MB-231, and retroviral packaging cell line Platinum-A were grown in Dulbecco's modified Eagle's medium (DMEM) supplemented with 10% fetal bovine serum and maintained at 37°C in an atmosphere containing 5% CO_2.

Antibodies and inhibitors

The antibodies used in this study were as follows: anti-FLAG antibody M2 (Sigma), anti-Mig-6 antibody PE-16 (Sigma), anti-Mig-6 antibody D-1 (Santa Cruz Biotechnology), anti-phospho-Chk1 (Ser-280) antibody (Cell Signaling), anti-Chk1 antibody G4 (Santa Cruz Biotechnology), anti-phospho-EGFR (Tyr-1068) antibody (Cell Signaling), anti-phospho-EGFR (Tyr-1173) antibody (Cell Signaling), anti-phospho-EGFR (Tyr-845) antibody (UPSTATE), anti-phospho-tyrosine antibody (4G10) (UPSTATE), anti-phospho-p44/p42 MAPK (Thr202/Thr204) antibody (Cell Signaling), anti-phospho-serine antibody (Invitrogen), anti-EGFR antibody (Santa Cruz Biotechnology), anti-ATM antibody (N-19) (Santa Cruz Biotechnology), anti-ATR antibody (2C1) (Santa Cruz Biotechnology), anti-phospho-Akt (Ser-473) antibody (587F11) (Cell Signaling), anti-Akt antibody (Cell Signaling), anti- phospho-p70S6K (Thr-389) antibody (Cell Signaling), anti-p70S6K antibody (Cell Signaling), anti-phospho-ERBB2 (Tyr-1248) antibody (UPSTATE), anti-ERBB2 antibody (Santa Cruz Biotechnology), anti-phospho-ERBB3 (Tyr-1289) antibody (Cell Signaling), anti-ERBB3 antibody (Santa Cruz Biotechnology), anti-β-actin antibody (Sigma), and anti-α-tubulin antibody DM1A (Sigma). The protein kinase inhibitors used in this study are indicated in Supplementary Table 1.

Plasmids and rec proteins

pBabe-EGFR was kindly provided by Wallice Langdon, School of Surgery and Pathology, University of Western Australia. A cDNA encoding WT Mig-6 cloned into pcDNA3.1 was described in a previous report (Tsunoda *et al*, 2002). All mutants of Mig-6 and Chk1 were constructed using standard rec DNA techniques. WT and mutant cDNA were re-cloned into the pGEX-6P-1 vector (Amersham) and the GST-Mig-6 fusion proteins were prepared as described previously (Frangioni and Neel, 1993). GST-tag was removed by PreScission Protease (GE Healthcare, Little Chalfont, UK) cleavage, and thereby Mig-6 proteins were eluted from Glutathione Sepharose 4B (GE Healthcare).

Immunoprecipitation

Cells were lysed in immunoprecipitation lysis buffer (0.5% Triton X-100, 300 mM NaCl, 25 mM Tris-HCl (pH 7.5)). Cell lysates were incubated with 2 μg of antibodies and protein G+ Sepharose 4FF (GE Healthcare) at 4°C for 2 h. Immunocomplexes were washed four times with lysis buffer, then denatured by treatment with an SDS sample buffer at 100°C for 5 min. IP samples, as well as the original cell lysates (input), were separated by SDS–PAGE and transferred from the gel onto a polyvinylidene difluoride (PVDF) membrane (Millipore, Billerica, MA), followed by IB. The proteins were visualized using an enhanced chemiluminescence system (Perkin Elmer, Waltham, MA).

Immunoblot analysis of phosphorylated proteins

We performed three methods to detect phosphorylation of Mig-6. The first was IB with anti-phospho-serine, anti-phospho-tyrosine, or anti-phospho-EGFR antibodies. The second was chemiluminescent detection using Phos-tag™ biotin (BTL; NARD Institute, Ltd.), which selectively binds to phosphorylated proteins blotted on PVDF membrane. Protein-blotted PVDF membrane was incubated with PB–SII solution (0.2 mM Phos-tag BTL, 0.4 mM $Zn(NO_3)_2$, 1 μl streptavidin-conjugated horseradish peroxidase in Tris-buffered saline/0.1% Tween) for 30 min at room temperature. Then, the membrane was washed and the chemiluminescence observed using ECL plus (GE Healthcare) on an X-ray film. The third method was the Phos-tag gel method, which can detect the mobility shifts of phosphorylated proteins using acrylamide-pendant Phos-tag (NARD Institute, Ltd.). The phosphate affinity SDS–PAGE was conducted with 25 μM Phos-tag acrylamide (AAL-107), 25 μM $MnCl_2$, 0.37 M Tris-HCl (pH 8.8), and 0.20% (w/v) SDS. After electrophoresis, the gel was soaked in a general transfer buffer containing 1 mM EDTA and then washed in the same transfer buffer without EDTA. After the treatment, it was transferred from the gel to PVDF membrane and immunoblotted with anti-Mig-6 antibody. The phosphorylated protein forms migrated more slowly than the non-phosphorylated forms.

In vitro phosphorylation assay

rec Mig-6 protein (0.1 μg) was incubated in 20 μl of kinase buffer (50 mM Tris-HCl (pH 7.5), 1 mM EGTA, 10 mM $MgCl_2$, 1 mM DTT) and ^{32}P-labelled ATP with or without 0.1 μg of purified rec GST-Chk1 kinase (Carna Biosciences, Kobe, Japan) at 30°C for 30 min with or without pretreatment with SB218078. The reaction was stopped by the addition of SDS sample buffer then analysed by 8% SDS–PAGE followed by autoradiography, or transferred to PVDF membrane and immunoblotted with anti-phospho-serine antibody.

RNA interference

MDA-MB-231 cells were transfected with human *Chk1* siRNA, *Mig-6* siRNA, or control siRNA oligonucleotides using Lipofectamine™ RNAiMAX (Invitrogen), according to the manufacturer's protocol. The nucleotide sequence of the *Chk1*(01) siRNA was 5′-GCGUGC CGUAGACUGUCCA-3′ and *Chk1*(04) siRNA was 5′-GAAGUUGG GCUAUCAAUGG-3′ with a 3′dTdT overhang. The nucleotide sequence of the human *Mig-6*(01) siRNA was 5′-CUACACUUUCUGAU